

**EXISTENCE, UNIQUENESS, AND NONUNIQUENESS OF
SINGLE-WAVE-FORM SOLUTIONS TO JOSEPHSON JUNCTION
SYSTEMS***

RENNIE MIROLLO[†] AND NED ROSEN[†]

Abstract. We study the existence and uniqueness of single-wave-form solutions for series arrays of N Josephson junctions coupled through general RLC loads. Our method recasts the conditions for a single-wave-form solution as a fixed point equation on a Hilbert space. We use this technique to prove that single-wave-form solutions exist when the bias current I is greater than 1 and are essentially unique when either N or I is large. We also employ these ideas to give explicit examples of series arrays which possess several distinct single-wave-form solutions.

Key words. Josephson junctions, single-wave-form solutions

AMS subject classifications. 34C25, 58F22

PII. S003613999834385X

1. Introduction. Josephson junctions are electronic superconducting devices capable of generating extremely high frequency voltage oscillations. Arrays of Josephson junctions coupled in various topologies have received much attention from both the mathematics and physics communities since these systems manifest rich dynamical behavior and are important in technological applications (see [L], [OD], and [VT]). We consider the case of a series array of N identical Josephson junctions coupled through an RLC load. The equations governing this system, expressed in dimensionless form, are

$$(1) \quad \begin{aligned} \beta\phi_j'' + \phi_j' + \sin \phi_j + Q' &= I, \\ LQ'' + RQ' + C^{-1}Q &= \frac{1}{N} \sum_{j=1}^N \phi_j'. \end{aligned}$$

We assume for simplicity that β, I, L, R, C are all *positive* constants (although our methods apply to some of the limiting cases where one or more of these constants is 0). We are concerned with the existence and uniqueness of *single-wave-form solutions* to (1). (These solutions are also called discrete rotating waves, ponies-on-a-merry-go-round, or splay-phase solutions in the literature.) Roughly speaking, these are periodic solutions to (1) where the functions ϕ_j are identical waveforms equally staggered in phase. More precisely, we define a single-wave-form solution (SWFS) to the system (1) to be a pair of C^∞ functions (ϕ, Q) such that for some $T > 0$,

$$\begin{aligned} \phi(t + T) &= \phi(t) + 2\pi, \\ Q(t + T) &= Q(t), \end{aligned}$$

and the functions $\phi_j(t) = \phi(t - \frac{j}{N}T)$, $j = 1, \dots, N$, and $Q(t)$ satisfy (1). Note that strictly speaking the function ϕ is not periodic, but can be considered periodic as a function from the reals \mathbb{R} to the circle $\mathbb{R}/2\pi\mathbb{Z}$. Then ϕ describes the motion of

*Received by the editors August 21, 1998; accepted for publication (in revised form) May 26, 1999; published electronically May 15, 2000.

<http://www.siam.org/journals/siap/60-5/34385.html>

[†]Boston College, Chestnut Hill, MA 02467-3806 (mirollo@bc.edu, rosen@bc.edu).

a particle on the circle which winds around the circle exactly once every period T . Aronson and Huang [AH2] call such a function ϕ a *running function*. (We remark that if (ϕ, Q) is an SWFS, then the functions ϕ and Q are in fact real analytic; this follows immediately from the fact that the differential equations (1) are real analytic, and therefore so is *any* solution to this system.)

The Josephson junction system is intimately related to the equation for a nonlinear forced pendulum

$$(2) \quad \beta\phi'' + \phi' + \sin\phi = I,$$

which has fairly simple dynamics for $I > 1$ (see [LHM] or [S] for a more elementary treatment). In fact, in a sense that we will make precise later, the nonlinear forced pendulum equation is the *limit* as $N \rightarrow \infty$ of the equation for SWFSs to the Josephson junction system (1). One of the goals of this paper is to provide an understanding of this relationship in detail, especially in cases where the two systems have essentially different behavior.

We choose to order the phase shifts to coincide with the numbering of the junctions. Of course, given any SWFS (ϕ, Q) we may produce a total of $N!$ solutions to (1) simply by reordering the phase shifts; among these $(N-1)!$ will be distinct up to time shift. We can also consider SWFSs where the junctions are divided into groups of M junctions where M is any divisor of N . Then we require that all junctions have identical waveforms, the junctions in each group are in phase, and the N/M groups are equally spaced in phase. However, it is easy to see that the equations for such an SWFS are identical to the system (1) with N replaced by N/M . In particular, when $M = N$ (all junctions are in phase) we are reduced to the system for $N = 1$. Hence we can focus our attention on the case of N junctions with N distinct phases with no loss of generality.

Our approach is to formulate the equations for an SWFS as a fixed point equation for the function ϕ in an appropriately chosen Hilbert space. We then apply this method in three ways. We begin by giving a simple proof of the existence of SWFSs. We then consider the question of uniqueness and use this method to establish two uniqueness theorems. Finally, we apply the fixed point methodology to give a numerical construction of multiple SWFSs. More precisely, we shall prove the following theorems.

THEOREM 1. *The Josephson junction system (1) admits an SWFS if $I > 1$.*

THEOREM 2. *There exists an I_0 depending only on L, R , and C such that the Josephson junction system (1) admits a unique SWFS for all $I \geq I_0$.*

THEOREM 3. *Fix any $\beta, I > 1, L, R$, and C . Then there exists an N_0 such that the Josephson junction system (1) admits a unique SWFS for all $N \geq N_0$.*

The first proof of Theorem 1 in full generality was given by Aronson and Huang in [AH2]. Before this, several special cases were established [AGM], [M]. The proof given by Aronson and Huang employs a homotopy argument that essentially connects the Josephson junction system to the nonlinear forced pendulum equation. It is known that the pendulum equation has a unique periodic solution for $I > 1$ [LHM]. Aronson and Huang use Leray–Schauder degree theory to extend the existence of periodic solutions through the homotopy to conclude that SWFSs exist for (1).

Our existence proof differs in several key respects. Having reduced the equations for an SWFS to a fixed point equation on a Hilbert space, we can use the Schauder–Tychonoff fixed point theorem to conclude that solutions exist. (The Schauder–Tychonoff theorem is a generalization of the Brouwer fixed point theorem to Banach

spaces.) We do not use any results about the pendulum equation; in fact, our approach establishes the existence of periodic solutions for the pendulum problem.

Loosely speaking, Theorems 2 and 3 state that uniqueness holds as $I \rightarrow \infty$ or $N \rightarrow \infty$. Huang and Aronson proved Theorem 3 in [HA], after having established the special cases where either $L = R = 0$ or $L = C^{-1} = 0$ [AH1]. Theorem 2 is new. Of course, these theorems beg the question of whether uniqueness holds for all parameter choices in (1). We answer this in the negative by demonstrating that, in fact, multiple SWFSs do exist. To do this, we develop a numerical method for calculating SWFSs. The method is essentially a multidimensional Newton's method which finds the Fourier coefficients of an SWFS; it allows us to compute SWFSs even in cases where they are dynamically unstable.

In one version of this method, the period T of the SWFS is specified in advance, but I is not specified. This gives the value I as a function of T . As we will see later, by a careful choice of L , R , and C the Josephson junction equations can be made almost identical to the pendulum equation, except for a "spike" in the $\pm N$ th eigenvalues of the linear operator governing the equations. This spike causes a corresponding spike in the graph of I against the period T , which means that for some values of I multiple periods will exist. (We will explain this in much greater detail later in the paper.)

The organization of the paper is as follows. We begin with the formulation of our fixed point method, which is contained in the proof of Theorem 1. The next section is devoted to establishing the uniqueness results (Theorems 2 and 3). The final section describes our numerical work and includes examples of multiple SWFSs. We conclude with some suggestions for future research.

2. Existence results.

THEOREM 4. *The Josephson junction system (1) admits an SWFS if $I > 1$.*

Proof. We examine the conditions for a pair of functions (ϕ, Q) to be an SWFS for (1) and make some preliminary reductions. Let $T > 0$ and set $\omega = 2\pi/T$ (think of ω as frequency). We consider ω a variable; part of finding an SWFS will be finding a value of ω consistent with (1). Suppose (ϕ, Q) is an SWFS of period T . Then the function $\phi(t) - \omega t$ is periodic with period T , so we can express ϕ in the form

$$\phi(t) = \omega t + a_0 + \sum_{n \neq 0} a_n e^{in\omega t}.$$

ϕ is real-valued so $a_{-n} = \overline{a_n}$ for all n . If we replace $\phi(t)$ by a suitable phase shift $\phi(t - t_0)$, we can assume that $a_0 = 0$. Hence we can express ϕ in the form

$$\phi(t) = f(\omega t) + \omega t,$$

where f is C^∞ , f has period 2π , and

$$\langle f \rangle \stackrel{\text{def}}{=} \frac{1}{2\pi} \int_0^{2\pi} f(t) dt = 0.$$

Similarly, we express Q as

$$Q(t) = b_0 + \sum_{n \neq 0} b_n e^{in\omega t}.$$

We integrate the second equation in (1) from 0 to T to obtain

$$C^{-1}b_0 = \omega.$$

Hence $b_0 = C\omega$ is uniquely determined, and we may express Q in the form

$$Q(t) = g(\omega t) + C\omega,$$

where g (like f) is C^∞ , has period 2π , and satisfies $\langle g \rangle = 0$. f and g must satisfy the equations

$$\beta\omega^2 f''(\omega t) + \omega f'(\omega t) + \omega + \sin(f(\omega t) + \omega t) + \omega g'(\omega t) = I,$$

$$L\omega^2 g''(\omega t) + R\omega g'(\omega t) + C^{-1}g(\omega t) = \frac{\omega}{N} \sum_{j=1}^N f' \left(\omega \left(t - \frac{j}{N}T \right) \right).$$

We replace ωt by t and simplify to

$$\begin{aligned} &\beta\omega^2 f''(t) + \omega f'(t) + \omega g'(t) = I - \omega - \sin(f(t) + t), \\ (3) \quad &L\omega^2 g''(t) + R\omega g'(t) + C^{-1}g(t) = \frac{\omega}{N} \sum_{j=1}^N f' \left(t - \frac{2\pi j}{N} \right). \end{aligned}$$

Conversely, if $\omega > 0$, f and g are C^∞ , 2π -periodic with $\langle f \rangle = \langle g \rangle = 0$, and ω, f , and g satisfy (3), then we obtain an SWFS (ϕ, Q) by defining $\phi(t) = f(\omega t) + \omega t$, $Q(t) = g(\omega t) + C\omega$. Hence we are reduced to studying the equations (3) for ω, f , and g .

Next we will eliminate g from the equations by expressing g as a linear function of f . Put $f(t) = \sum_{n \neq 0} a_n e^{int}$, $g(t) = \sum_{n \neq 0} b_n e^{int}$. Plugging these into (3) gives

$$(4) \quad (-Ln^2\omega^2 + iRn\omega + C^{-1})b_n = in\omega\zeta_n a_n,$$

where

$$\begin{aligned} \zeta_n &= \frac{1}{N} \sum_{j=1}^N e^{-2\pi i j n / N} \\ &= \begin{cases} 0 & \text{if } n \not\equiv 0 \pmod{N}, \\ 1 & \text{if } n \equiv 0 \pmod{N}. \end{cases} \end{aligned}$$

Now observe that

$$\text{Im}(-Ln^2\omega^2 + iRn\omega + C^{-1}) = Rn\omega \neq 0$$

so we can use (4) to solve for b_n in terms of a_n :

$$b_n = in\omega\zeta_n(-Ln^2\omega^2 + iRn\omega + C^{-1})^{-1}a_n$$

for all $n \neq 0$. In particular, $b_n = 0$ if $n \not\equiv 0 \pmod{N}$. Note also that for $n \equiv 0 \pmod{N}$, we have

$$|b_n| \sim \frac{1}{n}|a_n|$$

as $n \rightarrow \pm\infty$. This means that given any C^∞ function $f(t) = \sum_{n \neq 0} a_n e^{int}$, we can define $g(t) = \sum_{n \neq 0} b_n e^{int}$ using the above formulas for b_n , and be assured that g is

also C^∞ . Furthermore, if f is real-valued, then so is g , since we have $b_{-n} = \overline{b_n}$. Note that g is constructed as a very simple linear function of f (diagonal with respect to the basis $\{e^{int}\}_{n \neq 0}$). Since this linear operator depends on ω , we express this relation as $g = \mathcal{A}_\omega f$.

We are now reduced to solving for ω and f . Our goal is to express the conditions for ω and f in the form of a fixed point equation for the pair (f, ω) . From (3) we have

$$\beta\omega^2 f''(t) + \omega f'(t) + \omega[\mathcal{A}_\omega f]'(t) = I - \omega - \sin(f(t) + t).$$

This equation allows us to express I in terms of ω and f . We integrate over $[0, 2\pi]$ to obtain

$$(5) \quad I = \omega + \frac{1}{2\pi} \int_0^{2\pi} \sin(f(t) + t) dt$$

which we prefer to write as

$$\omega = I - \langle \sin(f(t) + t) \rangle.$$

The equation for f reduces to

$$(6) \quad -\beta\omega^2 f''(t) - \omega f'(t) - \omega[\mathcal{A}_\omega f]'(t) = \sin(f(t) + t) - \langle \sin(f(t) + t) \rangle.$$

We want to invert the left side of this equation so as to obtain a fixed point equation for f . The left side of (6) is an unbounded linear operator of f with eigenvectors $\{e^{int}\}_{n \neq 0}$. The eigenvalues of this operator are

$$\mu_n(\omega) = \beta\omega^2 n^2 - in\omega$$

if $n \not\equiv 0 \pmod{N}$ and

$$\mu_n(\omega) = \beta n^2 \omega^2 - in\omega + n^2 \omega^2 (-Ln^2 \omega^2 + iRn\omega + C^{-1})^{-1}$$

if $n \equiv 0 \pmod{N}$, and $n \neq 0$. For $n \not\equiv 0 \pmod{N}$, we have

$$(7) \quad |\mu_n(\omega)| > \omega|n|.$$

If $n \equiv 0 \pmod{N}$ and $n > 0$, we observe that

$$\begin{aligned} \operatorname{Im}(-Ln^2 \omega^2 + iRn\omega + C^{-1}) &= Rn\omega > 0 \\ \Rightarrow \operatorname{Im}(n^2 \omega^2 (-Ln^2 \omega^2 + iRn\omega + C^{-1})^{-1}) &< 0. \end{aligned}$$

Hence $\operatorname{Im} \mu_n(\omega) < -n\omega$, and again we get $|\mu_n(\omega)| > n\omega$. The case where $n < 0$ is similar. It also follows from the observation that $\mu_{-n}(\omega) = \overline{\mu_n(\omega)}$. Therefore (7) holds for all $n \neq 0$, and consequently, $\mu_n(\omega) \neq 0$ for all $n \neq 0$. We also see that

$$\mu_n(\omega) \sim \beta n^2 \quad \text{as } n \rightarrow \pm\infty.$$

Hence we can conclude that

$$\inf_{n \neq 0} |\mu_n(\omega)| > \omega$$

for any $\omega > 0$. We set $\lambda_n(\omega) = \mu_n(\omega)^{-1}$. We can express $\lambda_n(\omega)$ in the form $r_1(n\omega)$ or $r_2(n\omega)$, where r_1 and r_2 are the rational functions defined on $\mathbb{R} - \{0\}$ given below (the choice depends on whether $n \equiv 0 \pmod N$):

$$(8) \quad \begin{aligned} r_1(x) &= (\beta x^2 - ix)^{-1} \\ r_2(x) &= (\beta x^2 - ix + x^2(-Lx^2 + iRx + C^{-1})^{-1})^{-1}. \end{aligned}$$

Define the linear operator \mathcal{L}_ω by the equation

$$\mathcal{L}_\omega \left(\sum_{n \neq 0} c_n e^{int} \right) = \sum_{n \neq 0} \lambda_n(\omega) c_n e^{int}.$$

We see from above that

$$\sup_{n \neq 0} |\lambda_n(\omega)| < \omega^{-1}$$

and so

$$\|\mathcal{L}_\omega\| < \omega^{-1}.$$

Therefore \mathcal{L}_ω is a bounded linear operator on the real Hilbert space

$$L_0^2 = \left\{ \sum_{n \neq 0} c_n e^{int} \mid c_{-n} = \overline{c_n}, \sum_{n \neq 0} |c_n|^2 < \infty \right\}.$$

L_0^2 is of course equivalent to the space of measurable square integrable functions with zero mean:

$$L_0^2 = \left\{ f : [0, 2\pi] \rightarrow \mathbb{R} \mid \langle f^2 \rangle < \infty, \langle f \rangle = 0 \right\}.$$

If $f \in L_0^2$, define $\mathcal{S}(f)(t)$ by the right-hand side of (6):

$$\mathcal{S}(f)(t) = \sin(f(t) + t) - \langle \sin(f(t) + t) \rangle.$$

Note that there is no dependence on ω . For C^∞ functions f , the equation (6) is equivalent to the equation

$$f = \mathcal{L}_\omega \mathcal{S}(f).$$

Furthermore, if $f \in L_0^2$ satisfies this equation, then f is in fact C^∞ . To see this, recall that for any fixed ω , the eigenvalues of \mathcal{L}_ω are of the form $\beta^{-1}n^{-2} + O(|n|^{-3})$ as $n \rightarrow \pm\infty$ (see (8)). This implies that the range of \mathcal{L}_ω consists of continuous functions and that \mathcal{L}_ω maps C^k functions to C^{k+2} functions. The map \mathcal{S} preserves C^k functions, so we can argue iteratively that any fixed point f must be C^k for all k .

We also define

$$\mathcal{S}_0(f) = \langle \sin(f(t) + t) \rangle.$$

Like \mathcal{S} , \mathcal{S}_0 does not depend on ω . Now we can express the equations for (f, ω) as

$$(9) \quad \begin{aligned} f &= \mathcal{L}_\omega \mathcal{S}(f), \\ \omega &= I - \mathcal{S}_0(f). \end{aligned}$$

This is the desired form of the equations for (f, ω) . We conclude that SWFSs for the original system (1) are in one-to-one correspondence with solutions of the fixed point equations above.

We must demonstrate that (9) has a fixed point assuming that $I > 1$. Let $X = L_0^2 \times [I - 1, I + 1]$ and define

$$\mathcal{F}(f, \omega) = (\mathcal{L}_\omega \mathcal{S}(f), I - \mathcal{S}_0(f))$$

for $(f, \omega) \in X$. Note that $-1 \leq \mathcal{S}_0(f) \leq 1$ so \mathcal{F} does indeed map X to itself. X can be thought of as a subset of the product $L_0^2 \times \mathbb{R}$ which is naturally a Hilbert space. We wish to apply the Schauder–Tychonoff fixed point theorem (see [Ru, p. 143]): Let K be a compact convex subset of a Banach space. Then any continuous $\mathcal{F} : K \rightarrow K$ has a fixed point. Therefore we must show that our map \mathcal{F} is continuous and that the image $\mathcal{F}(X)$ is contained in some compact convex set K (then \mathcal{F} maps K to itself and thus has a fixed point in K). The second assertion follows from the inequality (7) for $\mu_n(\omega)$: Since $\omega \geq I - 1$ on X , we have

$$|\lambda_n(\omega)| \leq \frac{1}{(I - 1)|n|}$$

for all $n \neq 0$ and for all $(f, \omega) \in X$. We also observe that all the Fourier coefficients of $\mathcal{S}(f)$ are bounded by 1 since $|\sin(x)| \leq 1$ for all x . Hence the Fourier coefficients (c_n) of $\mathcal{L}_\omega \mathcal{S}(f)$ satisfy

$$|c_n| \leq \frac{1}{(I - 1)|n|}.$$

The set $K \subset L_0^2$ given by

$$\left\{ \sum_{n \neq 0} a_n e^{int} \mid |a_n| \leq \frac{c}{|n|} \right\}$$

for any constant $c > 0$ is compact and convex in L_0^2 . So for $c = (I - 1)^{-1}$, we have

$$\mathcal{F}(X) \subseteq K \times [I - 1, I + 1]$$

which is compact and convex in $L_0^2 \times \mathbb{R}$. Now we'll prove that \mathcal{F} is continuous. In fact, the map \mathcal{F} is actually C^∞ . To see this, we consider the map $\omega \mapsto \mathcal{L}_\omega$ as a map from $[I - 1, I + 1]$ to the algebra B of bounded linear operators on the Hilbert space L_0^2 . The operator \mathcal{L}_ω is diagonal with respect to the Hilbert basis $\{e^{int}\}_{n \neq 0}$, with eigenvalues given by the functions $\lambda_n(\omega)$. Consider the subspace $B_0 \subset B$ of diagonal operators. The operator norm restricted to B_0 is

$$\|\mathcal{L}\| = \sup_n |\lambda_n|,$$

where \mathcal{L} has eigenvalues (λ_n) . Therefore the map $\omega \mapsto \mathcal{L}_\omega$ is C^∞ on the interval $[I - 1, I + 1]$ if and only if for all k the k th derivative functions $\lambda_n^{[k]}$ are *equicontinuous* on $[I - 1, I + 1]$. Recall that $\lambda_n(\omega)$ can be expressed in the form $r_1(n\omega)$ or $r_2(n\omega)$, where r_1 and r_2 are the rational functions defined above (8). Hence the derivatives of λ_n are given by

$$\lambda_n^{[k]}(\omega) = n^k r_i^{[k]}(n\omega),$$

where $i = 1$ or 2 depending on whether $n \equiv 0 \pmod N$. Each r_i has a zero of order 2 at infinity and a simple pole at 0 . Hence $r_i^{[k]}$ has a zero of order $k + 2$ at infinity and a pole of order $k + 1$ at 0 . Therefore $x^{k+2}r_i^{[k]}(x)$ is bounded on \mathbb{R} , so we have constants M_k such that

$$\left| r_i^{[k]}(x) \right| \leq M_k |x|^{-k-2}$$

for all $x \neq 0$. Hence

$$\left| \lambda_n^{[k]}(\omega) \right| \leq M_k n^{-2} \omega^{-k-2}$$

for all $\omega > 0$. So for any given k , the functions $\lambda_n^{[k]}$ converge to 0 uniformly on $[I - 1, I + 1]$, and so the family $\lambda_n^{[k]}$ is equicontinuous on $[I - 1, I + 1]$. Hence the map $\omega \mapsto \mathcal{L}_\omega$ is C^∞ . The other ingredients \mathcal{S} and \mathcal{S}_0 of the map \mathcal{F} are clearly C^∞ , so we conclude that the map \mathcal{F} is C^∞ .

Therefore the Schauder–Tychonoff fixed point theorem implies that \mathcal{F} must have at least one fixed point, and so we are done. \square

COROLLARY 5. *The nonlinear forced pendulum equation (2) has a periodic solution if $I > 1$.*

Proof. We can carry out an identical analysis as we did above for the equation

$$\beta\phi'' + \phi' + \sin \phi = I.$$

Write $\phi(t) = f(\omega t) + \omega t$, where $f \in L^2_0$; then f must satisfy

$$\beta\omega^2 f''(t) + \omega f'(t) = I - \omega - \sin(f(t) + t).$$

The difference is that $Q(t)$ and $g(t)$ are out of the picture. This is equivalent to the fixed point equations

$$(10) \quad \begin{aligned} f &= \mathcal{L}_{\omega, \infty} \mathcal{S}(f), \\ \omega &= I - \mathcal{S}_0(f), \end{aligned}$$

where now *all* eigenvalues of $\mathcal{L}_{\omega, \infty}$ are given by the formula

$$\lambda_n(\omega) = r_1(n\omega) = (\beta n^2 \omega^2 - in\omega)^{-1}.$$

The argument now proceeds exactly as before. \square

We momentarily denote the operator \mathcal{L}_ω considered in Theorem 1 by $\mathcal{L}_{\omega, N}$ to emphasize the dependence on N . Then $\mathcal{L}_{\omega, N}$ and $\mathcal{L}_{\omega, \infty}$ differ only in their eigenvalues at multiples of N . The estimate (7) gives

$$\|\mathcal{L}_{\omega, N} - \mathcal{L}_{\omega, \infty}\| \leq \frac{2}{(I - 1)N}$$

which shows that $\mathcal{L}_{\omega, \infty}$ is the limit of $\mathcal{L}_{\omega, N}$ as $N \rightarrow \infty$. Hence the pendulum problem can be thought of as the $N \rightarrow \infty$ limit of the SWFS equation for the Josephson junction system. This observation will be discussed further during the proof of Theorem 3.

The existence of periodic solutions to the pendulum equation can of course be proved by more elementary means; see [LHM] or [S].

3. Uniqueness results.

PROPOSITION 6. *The equation $f = \mathcal{L}_\omega \mathcal{S}(f)$ has a unique solution for any $\omega \geq 1$.*

Proof. Recall that $\|\mathcal{L}_\omega\| < \omega^{-1}$, so $\|\mathcal{L}_\omega\| < 1$ when $\omega \geq 1$. Hence \mathcal{L}_ω is a contraction operator. It is also easy to see that \mathcal{S} does not increase distances on L_0^2 : We express \mathcal{S} as the composition of three functions on L^2 , namely $f(t) \mapsto f(t) + t$ (a translation given by adding the function $i(t) = t$), $f \mapsto \sin(f)$, and finally $f \mapsto \pi_0(f)$, where π_0 is orthogonal projection onto the subspace L_0^2 . Each of these functions clearly does not increase L^2 distances. Hence the composition $\mathcal{L}_\omega \mathcal{S}$ is a contraction map on L_0^2 for all $\omega \geq 1$ and the contraction mapping theorem implies that there is a unique function f_ω that satisfies the equation $f = \mathcal{L}_\omega \mathcal{S}(f)$. \square

We remark that the Schauder–Tychonoff fixed point argument in the proof of Theorem 1 applies to the simpler equation $f = \mathcal{L}_\omega \mathcal{S}(f)$, so this equation has at least one solution for any $\omega > 0$. Therefore given any parameters β, R, L, C, N , and ω (all positive) there exists at least one I such that the Josephson junction system (1) admits an SWFS with frequency ω . In other words, the system (1) *with unspecified* I admits at least one SWFS with any given frequency $\omega > 0$. Proposition 6 says that this SWFS is unique when $\omega \geq 1$. The point here is that Proposition 6 does not imply that (1) has a unique SWFS, even for $\omega \geq 1$, since it is possible that there may exist two SWFSs with distinct frequencies ω which determine the same value I . In other words, if we think of I as a function of ω , then the function $I(\omega)$ may not be monotonic. However if we can show that $I(\omega)$ is monotonic, then we do get uniqueness of SWFSs. This is the idea behind our next theorem.

THEOREM 7. *There exists an I_0 depending only on L, R , and C such that the Josephson junction system (1) admits a unique SWFS for all $I \geq I_0$.*

Proof. Let $\omega \geq 1$, and let f_ω be the unique solution to the equation $f = \mathcal{L}_\omega \mathcal{S}(f)$ given by Proposition 6. We wish to prove that the map $\omega \mapsto f_\omega$ is C^∞ . The implicit function theorem for Banach spaces applies to the equation $f = \mathcal{L}_\omega \mathcal{S}(f)$ since the map $\omega \mapsto \mathcal{L}_\omega$ is C^∞ and the norm of the derivative satisfies

$$\|\mathcal{L}_\omega D\mathcal{S}(f)\| \leq \|\mathcal{L}_\omega\| \|D\mathcal{S}(f)\| < 1.$$

Here $D\mathcal{S}(f)$, the Banach space derivative of \mathcal{S} at f , is the linear operator given by

$$D\mathcal{S}(f)g(t) = \cos(f(t) + t)g(t) - \langle \cos(f(t) + t)g(t) \rangle$$

for any $g \in L_0^2$. $\|D\mathcal{S}(f)\| \leq 1$ since \mathcal{S} does not expand L^2 distances. We conclude that the map $\omega \mapsto f_\omega$ is in fact C^∞ . Now consider the original system (1), but imagine that the constant I is not specified in advance. Then for any $\omega \geq 1$ there is a unique SWFS with frequency ω for (1) (unique of course up to phase shifts). This SWFS will determine a value of the constant I which depends smoothly on ω , so we write this as $I = I(\omega)$. (Since I and ω differ by the average of $\sin(f_\omega(t) + t)$ we also see that

$$\omega - 1 \leq I(\omega) \leq \omega + 1.$$

Therefore the range of the function $I(\omega)$ on the interval $[1, \infty)$ must contain the interval $[2, \infty)$. This gives an alternate proof of the existence of an SWFS for (1) for any $I \geq 2$.)

Now let $\omega > 1$. We differentiate the equation $f_\omega = \mathcal{L}_\omega \mathcal{S}(f_\omega)$ with respect to ω to obtain

$$\dot{f}_\omega = \dot{\mathcal{L}}_\omega \mathcal{S}(f_\omega) + \mathcal{L}_\omega D\mathcal{S}(f_\omega) \dot{f}_\omega,$$

where the dot denotes differentiation with respect to ω . Taking norms in the equation above gives

$$\|\dot{f}_\omega\| \leq \|\dot{\mathcal{L}}_\omega\| \|\mathcal{S}(f_\omega)\| + \|\mathcal{L}_\omega\| \|D\mathcal{S}(f_\omega)\| \|\dot{f}_\omega\|.$$

We know that both $\|\mathcal{S}(f_\omega)\| \leq 1$ and $\|D\mathcal{S}(f_\omega)\| \leq 1$. Hence

$$\|\dot{f}_\omega\| \leq \|\dot{\mathcal{L}}_\omega\| + \|\mathcal{L}_\omega\| \|\dot{f}_\omega\|.$$

$\|\mathcal{L}_\omega\| \leq \omega^{-1}$, so we can solve to obtain

$$\|\dot{f}_\omega\| \leq (1 - \|\mathcal{L}_\omega\|)^{-1} \|\dot{\mathcal{L}}_\omega\| \leq \left(\frac{\omega}{\omega - 1}\right) \|\dot{\mathcal{L}}_\omega\|.$$

We will need the result that $\|\dot{f}_\omega\| < 1$ for ω sufficiently large, and so we must estimate $\|\dot{\mathcal{L}}_\omega\|$. The eigenvalues of the operator $\dot{\mathcal{L}}_\omega$ are just the derivatives $\lambda'_n(\omega)$, and so $\|\dot{\mathcal{L}}_\omega\|$ is the supremum of $|\lambda'_n(\omega)|$ over all $n \neq 0$. We saw in the proof of Theorem 1 that there exists a constant M_1 such that

$$|\lambda'_n(\omega)| \leq M_1 n^{-2} \omega^{-3}.$$

Unfortunately, M_1 may depend on β as well as L, R , and C , so we have to work a little harder to eliminate the dependence on β . We claim that there exists an ω_0 depending only on L, R , and C such that

$$|\lambda'_n(\omega)| \leq \frac{16}{\omega^2}$$

for all n and $\omega \geq \omega_0$. We also require that $\omega_0 \geq 5$. Assuming this claim for the moment, we see that for $\omega \geq \omega_0$ we have

$$\|\dot{f}_\omega\| \leq \frac{16}{\omega(\omega - 1)} < 1.$$

To complete the proof, we differentiate the function $I(\omega)$ with respect to ω . $I(\omega)$ is given by (5) which gives

$$I'(\omega) = 1 + \langle \cos(f_\omega(t) + t) \dot{f}_\omega(t) \rangle.$$

The Cauchy–Schwarz inequality gives

$$|\langle \cos(f_\omega(t) + t) \dot{f}_\omega(t) \rangle| \leq \|\cos(f_\omega(t) + t)\|^{1/2} \|\dot{f}_\omega\|^{1/2} < 1.$$

Hence $I'(\omega) > 0$ for all $\omega \geq \omega_0$. This in turn implies that there is a unique SWFS for any $I \geq \omega_0 + 1$. (Otherwise for some $I \geq \omega_0 + 1$ there exist two distinct SWFSs. Since ω and I can differ by at most 1, the frequencies ω_1 and ω_2 of these SWFSs cannot be less than ω_0 . Hence we have two distinct values $\omega_2 > \omega_1 \geq \omega_0$ such that $I(\omega_1) = I(\omega_2)$, but this violates the condition $I'(\omega) > 0$ for all $\omega \geq \omega_0$.)

Now we establish the claim made earlier. Recall that we express $\lambda_n(\omega) = r_i(n\omega)$, $i = 1, 2$ (see (8)). It suffices to prove that there exists an x_0 such that

$$|r'_i(x)| \leq \frac{16}{x^2}$$

for $|x| \geq x_0$. First consider $r_1(x) = (\beta x^2 - ix)^{-1}$:

$$r_1'(x) = -(2\beta x - i)(\beta x^2 - ix)^{-2}$$

so

$$\begin{aligned} |r_1'(x)| &= \frac{|2\beta x - i|}{|\beta x^2 - ix|^2} = \frac{|2\beta x + i|}{x^2|\beta x + i|^2} \\ &\leq \frac{|2\beta x + 2i|}{x^2|\beta x + i|^2} = \frac{2}{x^2|\beta x + i|} \\ &\leq \frac{2}{x^2}. \end{aligned}$$

This proves the claim for $r_1(x)$. Write

$$r_2(x) = (\beta x^2 - ix + r_3(x))^{-1},$$

where

$$r_3(x) = x^2(-Lx^2 + iRx + C^{-1})^{-1}.$$

We see that $r_3(x) \rightarrow -L^{-1}$ and $r_3'(x) \rightarrow 0$ as $|x| \rightarrow \infty$. Hence there exists an x_0 such that $|x| \geq x_0$ implies

$$|r_3(x)| \leq \frac{1}{2}|x| \quad \text{and} \quad |r_3'(x)| \leq 1.$$

Observe that $|x| \leq |\beta x^2 - ix|$ and $1 \leq |2\beta x - i|$ for any β and x , so for $|x| \geq x_0$ we have

$$|r_3(x)| \leq \frac{1}{2}|\beta x^2 - ix| \quad \text{and} \quad |r_3'(x)| \leq |2\beta x - i|.$$

Now

$$r_2'(x) = -(2\beta x - i + r_3'(x))(\beta x^2 - ix + r_3(x))^{-2}.$$

If $|x| \geq x_0$, we obtain the inequalities

$$|2\beta x - i + r_3'(x)| \leq |2\beta x - i| + |r_3'(x)| \leq 2|2\beta x - i|$$

and

$$|\beta x^2 - ix + r_3(x)| \geq |\beta x^2 - ix| - |r_3(x)| \geq \frac{1}{2}|\beta x^2 - ix|.$$

Hence

$$|r_2'(x)| \leq \frac{2|2\beta x - i|}{(\frac{1}{2}|\beta x^2 - ix|)^2} = \frac{8|2\beta x - i|}{|\beta x^2 - ix|^2} = 8|r_1'(x)|.$$

Therefore

$$|r_2'(x)| \leq \frac{16}{x^2}$$

if $|x| \geq x_0$. \square

COROLLARY 8. *There exists an I_0 such that the nonlinear forced pendulum equation (2) has a unique periodic solution if $I \geq I_0$.*

Proof. The arguments in Theorem 2 apply to the operator $\mathcal{L}_{\omega, \infty}$ defined in the proof of Corollary 5. \square

This result is provisional since we will soon prove that the pendulum equation has a unique periodic solution if $I > 1$ (see Corollary 14). Our approach here has been to fix an ω , solve for the unique SWFS with frequency ω without specifying I in advance, and then argue that I depends monotonically on ω . This may seem somewhat roundabout, but there is a reason that the more direct approach fails: The map \mathcal{F} , in which both f and ω are variables, is not a contraction mapping on its domain. To see this, note that the derivative of the term \mathcal{S}_0 is given by

$$D\mathcal{S}_0(f)g = \langle \cos(f(t) + t)g(t) \rangle.$$

Since $|\cos(f(t) + t)| \leq 1$ we have $\|D\mathcal{S}_0\| \leq 1$. Define

$$f(t) = \begin{cases} -t & \text{if } 0 \leq t < \pi/2, \\ \pi - t & \text{if } \pi/2 \leq t < 3\pi/2, \\ 2\pi - t & \text{if } 3\pi/2 \leq t < 2\pi. \end{cases}$$

Then $\langle f \rangle = 0$ so $f \in L_0^2$. Let $g(t) = \cos(f(t) + t)$. Then

$$g(t) = \begin{cases} 1 & \text{if } 0 \leq t < \pi/2, \\ -1 & \text{if } \pi/2 \leq t < 3\pi/2, \\ 1 & \text{if } 3\pi/2 \leq t < 2\pi. \end{cases}$$

Hence $g \in L_0^2$ as well and $\|g\| = 1$. For this choice of f and g

$$D\mathcal{S}_0(f)g = \langle g^2 \rangle = \|g\|^2 = 1.$$

Hence $\|D\mathcal{S}_0(f)\| = 1$, so \mathcal{S}_0 is not a contraction. However, it is possible to analyze the fixed points of the function \mathcal{F} as $N \rightarrow \infty$ to obtain a uniqueness result. We do this in our next theorem.

THEOREM 9. *Fix any $\beta, I > 1, L, R$, and C . Then there exists an N_0 such that the Josephson junction system (1) admits a unique SWFS for all $N \geq N_0$.*

To prove this result we show that as $N \rightarrow \infty$ the equations (9) that determine the SWFSs converge to the equations (10) for periodic solutions to the pendulum problem. These equations (in our Hilbert space setting) have a unique, nondegenerate fixed point, so as $N \rightarrow \infty$ the same is true for the SWFS equations. We will need a few lemmas from calculus on Banach spaces. These are fairly standard results, but we include the proofs in an appendix for the convenience of the reader. We begin with a definition.

DEFINITION 10. *Let $F : U \rightarrow X$ be a continuously differentiable map, where U is an open subset of a Banach space X . $x_0 \in U$ is a nondegenerate fixed point of F if $F(x_0) = x_0$ and $\mathcal{I} - DF(x_0)$ has a bounded inverse.*

Here $\mathcal{I} : X \rightarrow X$ is the identity map. If X is finite-dimensional, then x_0 is nondegenerate if and only if the Jacobian matrix $DF(x_0)$ does not have 1 as an eigenvalue. We now state our lemmas.

LEMMA 11. *Let $F_n, F : U \rightarrow K \subset U$ be continuously differentiable maps, where K is compact and U is an open subset U of a Banach space X . Assume $F_n \rightarrow F$ and $DF_n \rightarrow DF$ uniformly on U . Suppose that F has a unique fixed point, which is nondegenerate. Then F_n has a unique fixed point for all sufficiently large n .*

LEMMA 12. Let $F : U \times (a, b) \rightarrow K \subset U$ be a continuously differentiable map, where K is compact and U is an open subset of a Banach space X . For any $c \in (a, b)$, define $F_c : U \rightarrow K$ by the rule $F_c(x) = F(x, c)$. Suppose all fixed points of F_c are nondegenerate for all $c \in (a, b)$. Then the number of fixed points of F_c is finite and constant as a function of c .

We also need a proposition on the fixed points of the pendulum problem.

PROPOSITION 13. All fixed points of the nonlinear forced pendulum equations (10) with $I > 1$ are nondegenerate.

We remark that this proposition is not immediately apparent even if one takes for granted the fact that for $I > 1$ the pendulum equation has a unique periodic orbit which is always attracting. We still must verify that the associated purely periodic function that satisfies our fixed point equations is nondegenerate. As we shall see, however, the required calculations are closely related to the Floquet equations for the pendulum problem.

Proof of Proposition 13. The periodic solutions to the pendulum problem correspond to solutions of the fixed point equation

$$(f, \omega) = \mathcal{F}_\infty(f, \omega) = (\mathcal{L}_{\omega, \infty} \mathcal{S}(f), I - \mathcal{S}_0(f))$$

that we considered in the proof of Corollary 5. (We use the notation \mathcal{F}_∞ here to distinguish this map from the equation for SWFs to the Josephson junction system (1), which we shall subsequently denote as \mathcal{F}_N .) We examine the conditions for a vector $(h, \eta) \in L_0^2 \times \mathbb{R}$ to be a solution to the linear equation

$$(11) \quad (h, \eta) = D\mathcal{F}(f, \omega)(h, \eta),$$

where (f, ω) is a fixed point for the map \mathcal{F}_∞ . Note that $D\mathcal{F}$ is a compact operator, and therefore to prove that $I - D\mathcal{F}(f, \omega)$ is invertible, it suffices to prove that the kernel of $I - D\mathcal{F}(f, \omega)$ is $\{0\}$; i.e., to prove that (11) above has no nontrivial solutions. (h, η) must satisfy the equations

$$(12) \quad \begin{aligned} h &= \mathcal{L}_{\omega, \infty} D\mathcal{S}(f)h + \dot{\mathcal{L}}_{\omega, \infty} \mathcal{S}(f)\eta, \\ \eta &= -D\mathcal{S}_0(f)h. \end{aligned}$$

There are two essentially different cases to consider: $\eta = 0$ and $\eta \neq 0$. Let's assume $\eta = 0$ first. Then the equations reduce to

$$\begin{aligned} h &= \mathcal{L}_{\omega, \infty} D\mathcal{S}(f)h, \\ 0 &= D\mathcal{S}_0(f)h. \end{aligned}$$

The first equation is equivalent to

$$\beta\omega^2 h''(t) + \omega h'(t) + (\cos(f(t) + t)) h(t) = \text{constant}$$

and the second equation gives $\langle \cos(f(t) + t)h(t) \rangle = 0$. Together these give

$$(13) \quad \beta\omega^2 h''(t) + \omega h'(t) + (\cos(f(t) + t)) h(t) = 0,$$

since $\langle h'' \rangle = \langle h \rangle = 0$. Now f satisfies the pendulum equation

$$\beta\omega^2 f''(t) + \omega f'(t) + \sin(f(t) + t) = I - \omega$$

and so

$$\beta\omega^2 f'''(t) + \omega f''(t) + (\cos(f(t) + t))(f'(t) + 1) = 0.$$

Hence $f' + 1$ satisfies (13) above. This makes sense, since (13) is just the linearization of the pendulum equation around the solution $f(t) + t$. Equation (13) is a second-order linear equation and thus has two linearly independent solutions. The Wronskian of (13) is given by

$$W(t) = W(0)e^{-(\beta\omega)^{-1}t}$$

which is not periodic. Hence h and $f' + 1$ must be linearly dependent, for otherwise h and $f' + 1$ would form a basis for all solutions and then $W(t)$ would be periodic. But now $\langle h \rangle = 0$ and $\langle f' + 1 \rangle = 1$, and so we must have $h = 0$. This completes the case when $\eta = 0$.

Now suppose $\eta \neq 0$. Since (12) is a linear equation, we can assume without loss of generality that $\eta = 1$. Then (12) reduces to

$$\begin{aligned} h &= \mathcal{L}_{\omega,\infty} D\mathcal{S}(f)h + \dot{\mathcal{L}}_{\omega,\infty} \mathcal{S}(f), \\ 1 &= -D\mathcal{S}_0(f)h. \end{aligned}$$

We will show that no function h can satisfy these equations. $\dot{\mathcal{L}}_{\omega,\infty}$ has eigenvalues $\lambda'_n(\omega)$, given by

$$\begin{aligned} \lambda'_n(\omega) &= -(2\beta\omega n^2 - in)(\beta\omega^2 n^2 - in\omega)^{-2} \\ &= (-2\beta\omega n^2 + in)\lambda_n(\omega)^2. \end{aligned}$$

Hence

$$\dot{\mathcal{L}}_{\omega,\infty} = (2\beta\mathcal{D}^2 + \mathcal{D})\mathcal{L}_{\omega,\infty}^2,$$

where \mathcal{D} denotes the linear operator given by the ordinary derivative $\mathcal{D}h = h'$. Since f satisfies the fixed point equation (10) we have $\mathcal{L}_{\omega,\infty}\mathcal{S}(f) = f$. Observe that $\mathcal{L}_{\omega,\infty}$, $\dot{\mathcal{L}}_{\omega,\infty}$, and \mathcal{D} all commute with each other since each of these operators is diagonal with respect to the basis $\{e^{int}\}_{n \neq 0}$. Substituting in (12) gives

$$h = \mathcal{L}_{\omega,\infty}(D\mathcal{S}(f)h + 2\beta\omega f'' + f').$$

(Here we use that $\mathcal{L}_{\omega,\infty}\mathcal{S}(f) = f$.) Inverting $\mathcal{L}_{\omega,\infty}$ yields

$$-\beta\omega^2 h''(t) - \omega h'(t) = \cos(f(t) + t)h(t) - \langle \cos(f(t) + t) \rangle h(t) + 2\beta\omega f''(t) + f'(t).$$

We have $D\mathcal{S}_0(f)h = \langle \cos(f(t) + t) \rangle h(t) = -1$ by (12), so we obtain

$$(14) \quad \beta\omega^2 h''(t) + \omega h'(t) + \cos(f(t) + t)h(t) + 2\beta\omega f''(t) + f'(t) + 1 = 0.$$

Now let $\tilde{h}(t) = h(t) + \omega^{-1}t(f'(t) + 1)$. We have

$$\begin{aligned} \tilde{h}'(t) &= h'(t) + \omega^{-1}(f'(t) + 1 + tf''(t)), \\ \tilde{h}''(t) &= h''(t) + \omega^{-1}(2f''(t) + tf'''(t)). \end{aligned}$$

Therefore

$$\begin{aligned} & \beta\omega^2\tilde{h}''(t) + \omega\tilde{h}'(t) + \cos(f(t) + t)\tilde{h}(t) \\ &= \beta\omega^2h''(t) + \omega h'(t) + \cos(f(t) + t)h(t) + 2\beta f''(t) + f'(t) + 1 \\ &= 0. \end{aligned}$$

(The terms with the factor t add up to

$$\beta\omega^2 f'''(t) + \omega f''(t) + \cos(f(t) + t)(f'(t) + 1) = 0$$

since $f' + 1$ satisfies (13).) Hence \tilde{h} satisfies the linearized pendulum equation (13). Now we have two solutions to (13), namely \tilde{h} and $f' + 1$. Note that

$$\tilde{h}(t + 2\pi) - \tilde{h}(t) = 2\pi\omega^{-1}(f'(t) + 1).$$

We cannot have $f'(t) = -1$ for all t since $\langle f' \rangle = 0$. Hence $\tilde{h}(t + 2\pi) - \tilde{h}(t)$ is not identically 0, so \tilde{h} is not periodic. This implies that \tilde{h} and $f' + 1$ are linearly independent, and so we can compute the Wronskian of (13) using \tilde{h} and $f' + 1$. But the Wronskian of (13) is proportional to $e^{-\beta\omega^{-1}t}$, whereas the Wronskian determinant computed from \tilde{h} and $f' + 1$ can grow at most like a power of t (in fact an easy computation shows that the Wronskian of \tilde{h} and $f' + 1$ is periodic). This gives the desired contradiction, namely that no such function h exists, and so we are finished with this case. \square

COROLLARY 14. *The nonlinear forced pendulum equation (2) has a unique periodic solution if $I > 1$.*

Proof. We apply Lemma 12 to the map \mathcal{F}_∞ , where

$$\mathcal{F}_\infty(f, \omega) = (\mathcal{L}_{\omega, \infty}\mathcal{S}(f), I - \mathcal{S}_0(f)).$$

Notice that \mathcal{F}_∞ depends smoothly on the parameter I , which corresponds to c in Lemma 12. Fix any $I_1 > 1$. Corollary 8 tells us that we can find some $I_2 > I_1$ such that \mathcal{F}_∞ has a unique fixed point. Choose an open interval (a, b) containing I_1 and I_2 , with $a > 1$, and choose ω_0 such that $0 < \omega_0 < a - 1$. We take our open set to be $U = L_0^2 \times (\omega_0, \infty)$. If $I \in (a, b)$, then \mathcal{F}_∞ maps U to the compact set $K \times [a - 1, b + 1] \subset U$, where K is given by

$$\left\{ \sum_{n \neq 0} a_n e^{int} \mid |a_n| \leq \frac{1}{\omega_0 |n|} \right\}$$

(this follows from the eigenvalue estimate $|\lambda_n(\omega)| \leq |\omega|^{-1} \leq \omega_0^{-1}$). Now we apply Lemma 12: All fixed points of \mathcal{F}_∞ are nondegenerate by Proposition 13, so we conclude that there is a unique fixed point for \mathcal{F}_∞ for all $I \in (a, b)$, and in particular for I_1 . \square

This result, like Corollary 5 concerning existence, can also be proven by elementary geometric arguments (see [LHM] for more details). Again, the main point here was to verify the nondegeneracy of fixed points in our Hilbert space context. Finally we can put all our results together and prove Theorem 3.

Proof of Theorem 3. We apply Lemma 11 to the maps \mathcal{F}_N and \mathcal{F}_∞ , where

$$\mathcal{F}_N(f, \omega) = (\mathcal{L}_{\omega, N}\mathcal{S}(f), I - \mathcal{S}_0(f)).$$

We can fix $I > 1$, and let $U = L_0^2 \times (\omega_0, \infty)$, where we choose ω_0 such that $0 < \omega_0 < I - 1$. Then \mathcal{F}_N maps U to the compact set $K \times [I - 1, I + 1] \subset U$, where K is the same compact set as in Corollary 14 above. Proposition 13 and Corollary 14 tell us that \mathcal{F}_∞ has a unique nondegenerate fixed point. Now

$$\mathcal{F}_N(f, \omega) - \mathcal{F}_\infty(f, \omega) = ((\mathcal{L}_{\omega, N} - \mathcal{L}_{\omega, \infty})\mathcal{S}(f), 0)$$

so we see that

$$\|\mathcal{F}_N(f, \omega) - \mathcal{F}_\infty(f, \omega)\| \leq \|\mathcal{L}_{\omega, N} - \mathcal{L}_{\omega, \infty}\|$$

and

$$\|D\mathcal{F}_N(f, \omega) - D\mathcal{F}_\infty(f, \omega)\| \leq \|\mathcal{L}_{\omega, N} - \mathcal{L}_{\omega, \infty}\| + \|\dot{\mathcal{L}}_{\omega, N} - \dot{\mathcal{L}}_{\omega, \infty}\|$$

since $\|\mathcal{S}(f)\|, \|D\mathcal{S}(f)\| \leq 1$. Both $\|\mathcal{L}_{\omega, N} - \mathcal{L}_{\omega, \infty}\|$ and $\|\dot{\mathcal{L}}_{\omega, N} - \dot{\mathcal{L}}_{\omega, \infty}\|$ converge to 0 as $N \rightarrow \infty$, uniformly for $\omega > \omega_0$. Hence Lemma 11 applies, and we conclude that the Josephson junction system (1) has a unique SWFS if N is sufficiently large. \square

4. Numerical computations and nonuniqueness results. An SWFS for the Josephson junction system (1) corresponds to a fixed point (f, ω) of the operator $\mathcal{F}(f, \omega) = (\mathcal{L}_\omega \mathcal{S}(f), I - \mathcal{S}_0(f))$; for fixed ω and unspecified I , a fixed point f of $\mathcal{L}_\omega \mathcal{S}$ yields an SWFS for the system with $I = \omega + \mathcal{S}_0(f)$. In this section, we give numerical methods for finding truncated Fourier series approximations to fixed points of either \mathcal{F} or $\mathcal{L}_\omega \mathcal{S}$. We use these to verify that there exist parameters β, L, R , and C for which $I(\omega)$ is not monotonic; hence for some values of I the Josephson junction system with these given parameters admits SWFSs with distinct periods. Our approach uses Newton’s method, which unlike some numerical methods can find solutions regardless of whether they are dynamically stable or unstable. We begin with a brief description of it.

We approximate the 2π -periodic functions in L_0^2 by truncating their real Fourier series after M terms, so we consider functions of the form

$$f(t) = \sum_{j=1}^M a_j \cos(jt) + b_j \sin(jt).$$

These functions form a $2M$ -dimensional subspace of L_0^2 which we denote H_M . Identify H_M with \mathbb{R}^{2M} in the obvious way so that the function $f(t)$ is identified with the sequence $(a_1, b_1, \dots, a_M, b_M)$ of its Fourier coefficients. For f in H_M , let $\mathcal{S}_M(f)$ be the truncation, to H_M , of $\mathcal{S}(f)$; that is,

$$\mathcal{S}_M(f) = \sum_{j=1}^M c_j \cos(jt) + d_j \sin(jt),$$

where c_j and d_j can be computed numerically from the formulas

$$c_j = \frac{1}{\pi} \int_0^{2\pi} \sin(f(t) + t) \cos(jt) dt,$$

$$d_j = \frac{1}{\pi} \int_0^{2\pi} \sin(f(t) + t) \sin(jt) dt.$$

The linear operator \mathcal{L}_ω maps H_M to H_M ; we can express \mathcal{L}_ω in terms of the coordinate system chosen above by the formula

$$\mathcal{L}_\omega(c_1, d_1, \dots, c_M, d_M) = (A_1, B_1, \dots, A_M, B_M),$$

where $A_j = x_j c_j + y_j d_j$, $B_j = -y_j c_j + x_j d_j$, and x_j, y_j are given by $x_j + iy_j = \lambda_j(\omega)$, the j th eigenvalue of \mathcal{L}_ω .

Fix M and set $G_\omega = \mathcal{L}_\omega \mathcal{S}_M$, so $G_\omega : \mathbb{R}^{2M} \rightarrow \mathbb{R}^{2M}$. In order to find a fixed point of G_ω by Newton's method, iterate the function $v \mapsto V$ given by

$$V = v - (DG_\omega(v) - I_{2M})^{-1}(G_\omega(v) - v),$$

where $DG_\omega(v)$ denotes the Jacobian of G_ω at v and I_{2M} is the $2M \times 2M$ identity matrix. Since \mathcal{L}_ω is linear,

$$DG_\omega(v) = D(\mathcal{L}_\omega \mathcal{S}_M)(v) = \mathcal{L}_\omega D\mathcal{S}_M(v),$$

and the partial derivatives in the Jacobian $D\mathcal{S}_M(v)$ can be evaluated by numerical integration from the formula

$$\frac{\partial c_j}{\partial a_k} = \frac{1}{\pi} \int_0^{2\pi} \cos(f(t) + t) \cos(kt) \cos(jt) dt,$$

or similar formulas for the other partial derivatives. We note in passing that \mathcal{S}_M , viewed as a function on \mathbb{C}^M via truncated Fourier series, does not have holomorphic component functions; since the Jacobian of \mathcal{S}_M must be computed for Newton's method, it is in fact simpler, and no less efficient, to work with real Fourier coefficients in \mathbb{R}^{2M} .

For the operator \mathcal{F} , define a truncation $F_I : \mathbb{R}^{2M+1} \rightarrow \mathbb{R}^{2M+1}$ by

$$F_I(a_1, b_1, \dots, a_M, b_M, \omega) = (A_1, B_1, \dots, A_M, B_M, \Omega),$$

where the Fourier coefficients A_j and B_j are computed as they are for G_ω and the new frequency is given by

$$\Omega = I - \frac{1}{2\pi} \int_0^{2\pi} \sin(f(t) + t) dt.$$

The partials $\frac{\partial \Omega}{\partial a_k}$ or $\frac{\partial \Omega}{\partial b_k}$ in the Jacobian DF_I can be computed by numerical integration, and, since the operator \mathcal{S} is independent of ω , we have

$$\frac{\partial A_j}{\partial \omega} = c_j x'_j(\omega) + d_j y'_j(\omega)$$

and

$$\frac{\partial B_j}{\partial \omega} = -c_j y'_j(\omega) + d_j x'_j(\omega),$$

where

$$\lambda'_j(\omega) = x'_j(\omega) + iy'_j(\omega);$$

finally, $\frac{\partial \Omega}{\partial \omega} = 0$ since Ω does not depend on ω .

Given a particular parameter list, our approach is to use Newton's method on G_ω to find a fixed point f of $\mathcal{L}_\omega \mathcal{S}$, then compute $I = \omega + \mathcal{S}_0(f)$, at many values of ω .

For all $\omega > 0$, $\mathcal{L}_\omega\mathcal{S}$ has at least one fixed point (see Proposition 6 and the remark following it), and we use the notation $I(\omega)$ for the value of I so found, even though it may be possible that for small ω , $\mathcal{L}_\omega\mathcal{S}$ has multiple fixed points and hence $I(\omega)$ has multiple values. Strictly speaking, our method finds a *branch* $I(\omega)$ of the relation

$$\left\{(\omega, I) \mid I = \omega + \mathcal{S}_0(f) \text{ for some fixed point } f \text{ of } \mathcal{L}_\omega\mathcal{S}\right\}.$$

We do not know if there exist parameters for which $I(\omega)$ is multivalued, but we have found parameters for which $I(\omega)$ is nonmonotonic; a strategy for finding such parameters follows next.

Fix $\beta > 0$, and let $I_P(\omega)$ denote the value of I for which the forced pendulum equation (2) has a periodic solution with frequency ω . The function $I_P(\omega)$ is monotonic for any $\beta > 0$ (this is proved in [LHM]), so, to make $I(\omega)$ nonmonotonic for the Josephson junction system, we seek parameters β, L, R, C , and N which make the Josephson junction eigenvalue functions $\lambda_j(\omega) = r_2(j\omega)$ behave different from the corresponding pendulum eigenvalues $r_1(j\omega)$ for j divisible by N . Since

$$|r_1(x)| = |\beta x^2 - ix|^{-1} = \frac{1}{|x|\sqrt{\beta^2 x^2 + 1}}$$

is a decreasing function, a simple strategy is to arrange that

$$|r_2(x)| = |\beta x^2 - ix + x^2(-Lx^2 + iRx + C^{-1})^{-1}|^{-1}$$

be rapidly increasing on some interval $[x_0, x_1]$. Then for $j = kN$, $|\lambda_j(\omega)| = |r_2(kN\omega)|$ changes quickly with respect to ω for $kN\omega \in [x_0, x_1]$; thus we look for nonmonotonicity for $I(\omega)$ around the intervals $x_0/kN < \omega < x_1/kN$, $k = 1, 2, 3, \dots$

Choose $R \approx 0$; then the imaginary part of the *RLC* term in $r_2(x)$ is negligible, so

$$r_2(x) \approx (\beta x^2 - ix + x^2(-Lx^2 + C^{-1})^{-1})^{-1} = \frac{xZ(x) + i}{x(x^2Z(x)^2 + 1)},$$

where $Z(x) = \beta + (C^{-1} - Lx^2)^{-1}$. Let $x_0 = \sqrt{(LC)^{-1}}$, so $Z(x_0) = \infty$, and $x_1 = \sqrt{(LC)^{-1} + (L\beta)^{-1}}$, so $Z(x_1) = 0$. Then $x_0 < x_1$, $r_2(x_0) \approx 0$ and $r_2(x_1) \approx i/x_1$, so $|r_2(x)|$ increases from approximately 0 to $1/x_1$ on $[x_0, x_1]$. Choose L and β sufficiently large so that $x_1 - x_0$ is small and $1/x_1$ is not small; then $|r_2(x)|$ has large slope on $[x_0, x_1]$, as desired.

A straightforward situation occurs when $C \ll \beta \ll L$ (and $R \approx 0$); since $C^{-1} \gg \beta^{-1}$, then $x_0 \approx x_1$ and so $|r_2(x)|$ has a sharp spike on $[x_0, x_1]$, and for x away from the spike, $Z(x) \approx \beta$ and so $r_2(x) \approx r_1(x)$. Let $\omega_0 = x_0/N$; then, for values of ω which are not near ω_0/k ($k = 1, 2, 3, \dots$), all the Josephson junction eigenvalues $\lambda_j(\omega)$ are very close to the corresponding eigenvalues for the pendulum equation, so $I(\omega)$ will closely follow $I_P(\omega)$ except near the points ω_0/k . Example 15 illustrates this phenomenon.

We present two examples of parameter lists for which $I(\omega)$ is not monotonic and find, for each one, Fourier coefficients and frequencies for multiple SWFSs at a particular value of I . We also compare the values to those obtained from the corresponding forced pendulum equation; for clarity, the function $I(\omega)$ is labeled I_{JJ} in pictures displaying both I_{JJ} and I_P .

As we are mainly interested in the relationship between ω and I , we choose the truncation point M sufficiently large so that, for fixed ω (respectively I), the computed value of I (respectively ω) remains constant through five decimal places

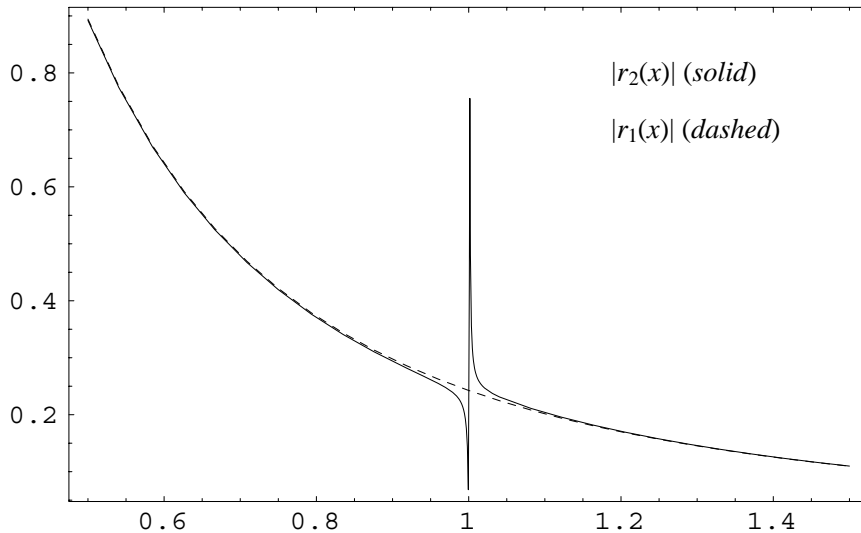


FIG. 1. Magnitudes of $r_1(x)$ and $r_2(x)$ on $[0.5, 1.5]$ for Example 15 ($\beta = 4$; $L = 100$, $R = 0.01$, $C = 0.01$). Since $R \approx 0$ and $C \ll \beta \ll L$, then $r_1(x) \approx r_2(x)$ except near the spike at $x = 1.00$. The spike is shown in Figure 2.

as M is increased; this amounts to the higher Fourier coefficients for the fixed point function $f(t)$ having decayed enough. For relatively large ω , the coefficients decay quickly and small values of M give very accurate results for $I(\omega)$, but larger (and larger) values of M are required for accurate computations as $\omega \rightarrow 0$.

In the examples below, the computations for the $I(\omega)$ graphs use Newton's method to find a fixed point f for G_ω at many values of ω in some interval $\omega_{\min} \leq \omega \leq \omega_{\max}$, starting at the largest value $\omega_{\max} > 1$ (convergence is assured for large ω from any initial coefficients since $\mathcal{L}_\omega \mathcal{S}$ is a contraction), then using each computed fixed point as the initial sequence of the iteration at the next (slightly smaller) frequency $\omega - \Delta\omega$. Generally, M is increased as ω gets smaller, and $\Delta\omega$ is decreased when $|I'(\omega)|$ is large. Having found multiple (f, ω) with nearly the same I , we fix I and iterate Newton's method for F_I , starting at each approximate pair (f, ω) found from the first computation, to get the Fourier coefficients and frequencies for the multiple SWFSs.

EXAMPLE 15. $\beta = 4$; $L = 100$, $R = 0.01$, $C = 0.01$; $N = 2$.

We have $x_0 = 1$ and $x_1 = 1.001249\dots$. Then $|r_2(x) - r_1(x)| < 0.02$ for $|x - 1| > 0.01$, but $r_2(x)$ spikes dramatically in $[x_0, x_1]$ (Figures 1 and 2). With $N = 2$, $\omega_0 = 1/2$ and $I(\omega)$ should follow $I_P(\omega)$ except near $\omega = 1/2k$. Figure 3 shows $I(\omega)$ for $0.14 < \omega < 0.7$; the spikes at $\omega = 1/2, 1/4, 1/6$ show that $I(\omega)$ is not monotonic and hence, for various values of I , the Josephson junction system with these parameters admits multiple SWFSs. The rectangle surrounding the spike at $\omega = 1/2$ in Figure 3 is blown up in Figure 4, which also shows $I_P(\omega)$ on the interval $[0.49, 0.51]$ ($I(\omega)$ and $I_P(\omega)$ are graphically indistinguishable away from the spikes in Figure 3).

The dots are drawn at $I = 0.7034$ in Figures 3 and 4; this Josephson junction system admits SWFSs with frequencies $\omega = 0.500560\dots$, $0.500759\dots$, and $0.599474\dots$, while the periodic pendulum solution with $\beta = 4$, $I = 0.7304$ has frequency $\omega = 0.599543\dots$. Table 1 lists the Fourier coefficients through $M = 8$

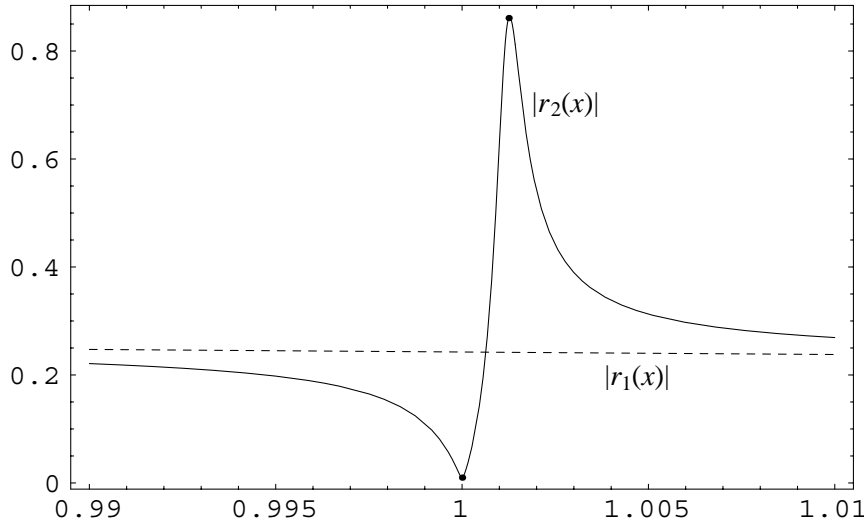


FIG. 2. The spike in $|r_2(x)|$ for Example 15. The dots are at $x_0 = \sqrt{(LC)^{-1}} = 1$ and $x_1 = \sqrt{(LC)^{-1} + (L\beta)^{-1}} = 1.00125$, between which $|r_2(x)|$ increases from 0.009893 to 0.86083.

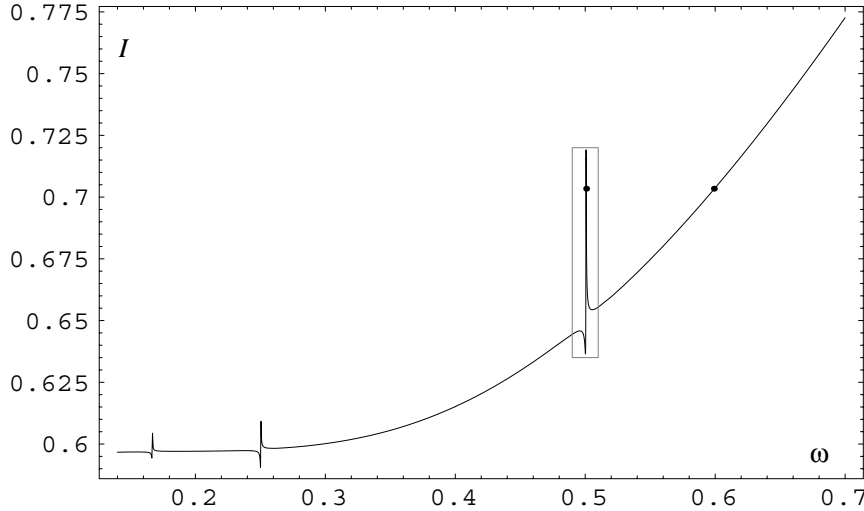


FIG. 3. $I(\omega)$, for $0.14 < \omega < 0.7$, for the Josephson junction system of Example 15: $\beta = 4$; $L = 100$, $R = 0.01$, $C = 0.01$; $N = 2$. The spikes at $\omega = 1/2, 1/4, 1/6$ reflect the spike at $x = 1.0$ in $|r_2(x)|$. The points on the graph are computed with $M = 5$ near $\omega = 0.7$, increasing to $M = 10$ for $0.14 < \omega < 0.24$; the sampling varies from $\Delta\omega = 0.01$ to $\Delta\omega = 0.0002$. At $I = 0.7034$ (the dots), there are three SWFSs with distinct frequencies, one near 0.6 and the other two on the spike near 0.5; the rectangle at $\omega = 0.5$ outlines the region which is shown on Figure 4.

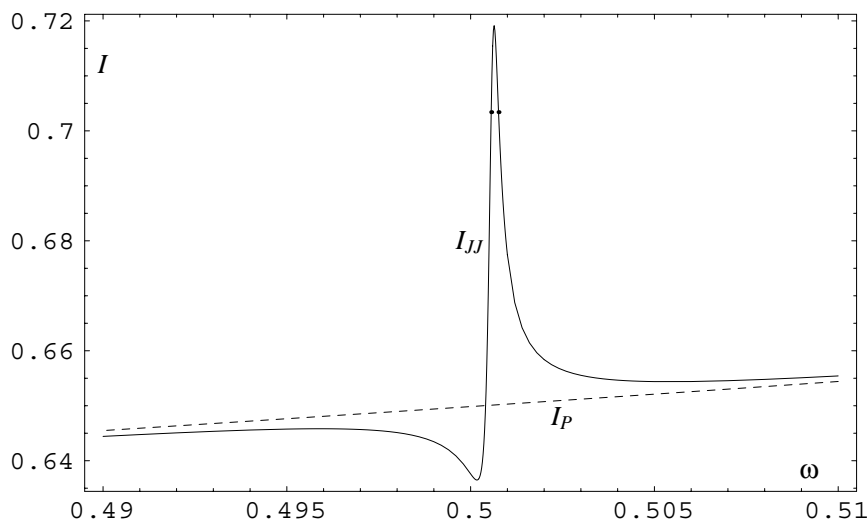


FIG. 4. The spike in $I(\omega)$, and $I_P(\omega)$, for $0.49 < \omega < 0.51$ (Example 15). The dots are at $I = 0.7034$, $\omega = 0.50056$, and $\omega = 0.50076$.

for all four of these waveforms $f(t)$; of course, the Josephson junction solution for $\omega = 0.599474$ is very close to the pendulum solution. The graph of the waveforms on $[0, 2\pi]$ in Figure 5 shows only three curves since, at the resolution of Figure 5, the pendulum waveform is identical to the Josephson junction waveform for $\omega = 0.599474$.

We conclude Example 15 by looking at the computations of the bias current I at $\omega = 0.14$ for various truncation points M . The graph in Figure 3 uses $M = 10$ pairs of Fourier coefficients to compute the fixed point $f(t)$ of $G_{0.14}$, from which $I(0.14) = 0.14 + (1/2\pi) \int_0^{2\pi} \sin(f(t) + t) dt$ amounts to 0.596676, which is sufficiently accurate, since the graph in Figure 3 does not change visibly when M is increased. With $M = 12$ and $M = 20$, the values obtained for $I(0.14)$ are 0.596920 and 0.596978, respectively. Table 2 shows the Fourier coefficients of $f(t)$ computed with $M = 12$ and $M = 20$; the coefficients at $\omega = 0.14$ decay much more slowly than those at, for example, $\omega = 0.5$ (Table 1), hence the larger number of terms required for accurate computation of I .

We make a final observation. If $I(0.14)$ is computed from the first twelve pairs of coefficients found with $M = 20$, the value obtained is 0.596977, which is much closer (within 0.000001) to the $M = 20$ value than the $M = 12$ value; the truncation errors in computing I lie mostly in the low order coefficients of the fixed point $f(t)$.

EXAMPLE 16. $\beta = 2$; $L = 1$, $R = 0.0001$, $C = 2$; $N = 1$.

In this case, $x_0 = \sqrt{0.5} = 0.707\dots$ and $x_1 = 1$. Again, $|r_2(x)|$ increases on $[x_0, x_1]$, but with β , L , and C of comparable magnitudes, the “spike” is gradual (Figure 6), and $|r_2(x) - r_1(x)|$ stays large on $[0, x_0]$ (Figure 7). In general, with $R \approx 0$,

$$\lim_{x \rightarrow 0} |r_2(x) - r_1(x)| \approx C,$$

so, with $C \gg 0$, as in this example, $r_2(x)$ and $r_1(x)$ will not be close on $[0, x_0]$. Of course, for x sufficiently large, $r_2(x) \approx r_1(x)$, and in the present case, $x > 2$ is sufficiently large.

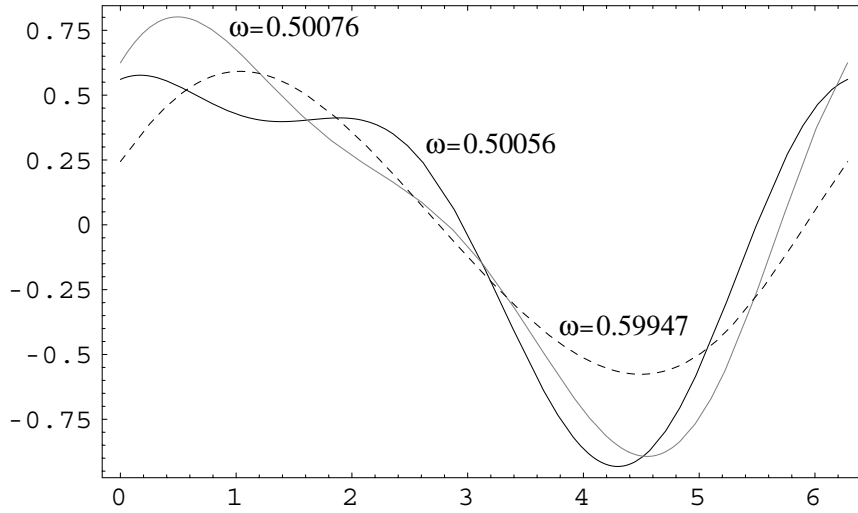


FIG. 5. Waveforms $f(t)$ on $[0, 2\pi]$, for the three SWFSs to the Josephson junction system with $\beta = 4$; $L = 100$, $R = 0.01$, $C = 0.01$; $I = 0.7034$; $N = 2$. The waveform for the periodic pendulum solution at $\beta = 4$, $I = 0.7034$ is indistinguishable from the Josephson junction waveform with frequency $\omega = 0.59947$ (dashed).

TABLE 1

Frequencies ω , and Fourier coefficients of the waveforms $f(t)$, for the three SWFSs of the Josephson junction system at $I = 0.7034$ with parameters in Example 15 ($\beta = 4$; $L = 100$, $R = 0.01$, $C = 0.01$; $N = 2$). The fourth column lists the data for the periodic solution of the forced pendulum equation with $\beta = 4$, $I = 0.7034$, which has frequency $\omega = 0.59954$, and is barely distinguishable from the Josephson junction SWFS with frequency $\omega = 0.59947$.

ω	0.50056	0.500759	0.599474	0.599543
a_1	0.348852	0.373158	0.214028	0.213913
b_1	0.589729	0.650548	0.540437	0.54033
a_2	0.197328	0.230408	0.025774	0.0255809
b_2	-0.177774	0.0437343	0.0386611	0.0384719
a_3	0.013806	0.0175377	0.00350038	0.00349019
b_3	-0.00862841	0.00268181	0.00314869	0.00314226
a_4	0.00126916	0.003048	0.000479481	0.00477182
b_4	-0.00269959	-0.00110916	0.000242377	0.000241693
a_5	-0.000311979	0.000411365	0.0000640179	0.0000636749
b_5	-0.000428752	-0.000562759	0.0000129231	0.0000129216
a_6	-0.000120056	0.0000180594	8.2529×10^{-6}	8.20199×10^{-6}
b_6	-0.000014295	-0.000145413	-5.91569×10^{-7}	-5.771×10^{-7}
a_7	-0.0000165272	-0.0000127883	1.01562×10^{-6}	1.00855×10^{-6}
b_7	0.0000136735	-0.000028396	-3.62801×10^{-7}	-3.58547×10^{-7}
a_8	-2.89591×10^{-7}	-5.46561×10^{-6}	1.17157×10^{-7}	1.16275×10^{-7}
b_8	4.55207×10^{-6}	-4.01106×10^{-6}	-8.27472×10^{-8}	-8.18185×10^{-8}

Since $N = 1$, the Josephson junction eigenvalues $\lambda_j(\omega)$ are just $r_2(\omega)$, which for $\omega > 2$, are very close to the corresponding pendulum eigenvalues $r_1(\omega)$; hence, for $\omega > 2$, $I(\omega)$ and $I_P(\omega)$ are virtually identical. As ω decreases from $\omega = 2$, the first eigenvalue $\lambda_1(\omega) = r_2(\omega)$ diverges from the first pendulum eigenvalue $r_1(\omega)$ and the function $I(\omega)$ similarly moves away from $I_P(\omega)$ (Figure 8). As ω decreases further, $I(\omega)$ shows no correlation with $I_P(\omega)$; for example, if $0.2 < \omega < 0.4$, $I_P(\omega)$ lies in

TABLE 2

Fourier coefficients of the SWFS waveform $f(t)$ with frequency $\omega = 0.14$ for the Josephson junction system of Example 15, computed with $M = 20$ and $M = 12$ (pairs of) coefficients. Note the slow decay rate for the coefficients compared to those in Table 1, where ω is near 0.5 and 0.6. The bias current $I = I(0.14)$ at this solution comes out to 0.596978 with $M = 20$ and 0.596920 with $M = 12$. If $I(0.14)$ is computed using only the first twelve from the $M = 20$ coefficients, the result is $I(0.14) = 0.596977$; hence the truncation error in $I(0.14)$ is almost all in the computation of the low order coefficients of the fixed point $f(t)$ rather than in the computation of I from $f(t)$.

j	$a_j(M = 20)$	$b_j(M = 20)$	$a_j(M = 12)$	$b_j(M = 12)$
1	1.04801	1.4478	1.0479	1.44787
2	0.62792	0.24302	0.62787	0.24311
3	0.30619	-0.05138	0.30618	-0.0513
4	0.11921	-0.09773	0.11922	-0.09767
5	0.02857	-0.075038	0.0286	-0.075004
6	-0.00669	-0.0422	-0.00666	-0.04218
7	-0.01489	-0.01824	-0.01485	-0.01823
8	-0.01239	-0.004605	-0.01236	-0.004614
9	-0.007296	0.00128	-0.007274	0.001261
10	-0.003225	0.002756	-0.003215	0.002729
11	-0.0007904	0.0023096	-0.007948	0.0022828
12	0.0002904	0.001391	0.0002756	0.001371
13	0.0005612	0.0006125		
14	0.0004688	0.0001411		
15	0.0002808	-0.00007012		
16	0.0001221	-0.00001213		
17	0.0000255	-0.00009938		
18	-0.00001735	-0.00005891		
19	-0.00002702	-0.000025016		
20	-0.000021653	-4.60286×10^{-6}		

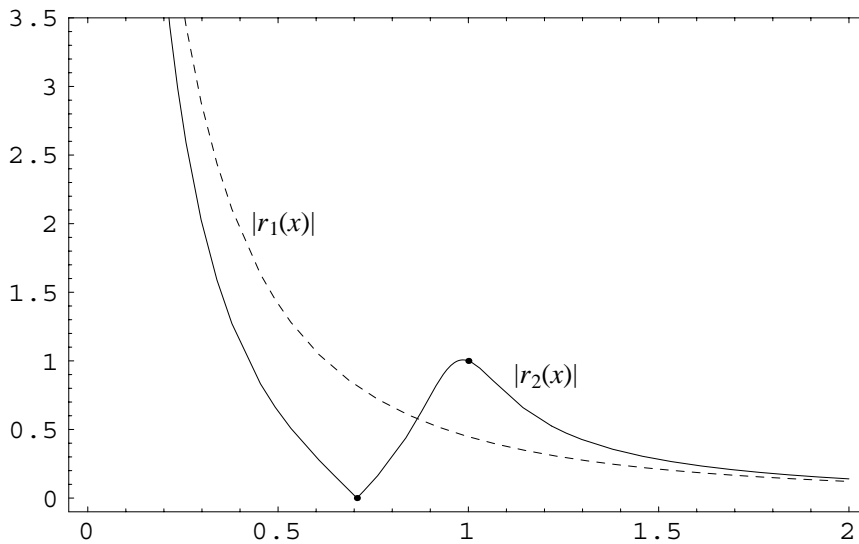


FIG. 6. $|r_1(x)|$ and $|r_2(x)|$ for Example 16 ($\beta = 2$; $L = 1$, $R = 0.0001$, $C = 2$) on $[0.2, 2]$, showing the points at x_0 and x_1 (the dots): $(0.7071, 0.00014)$ and $(1.00, 0.9996)$.

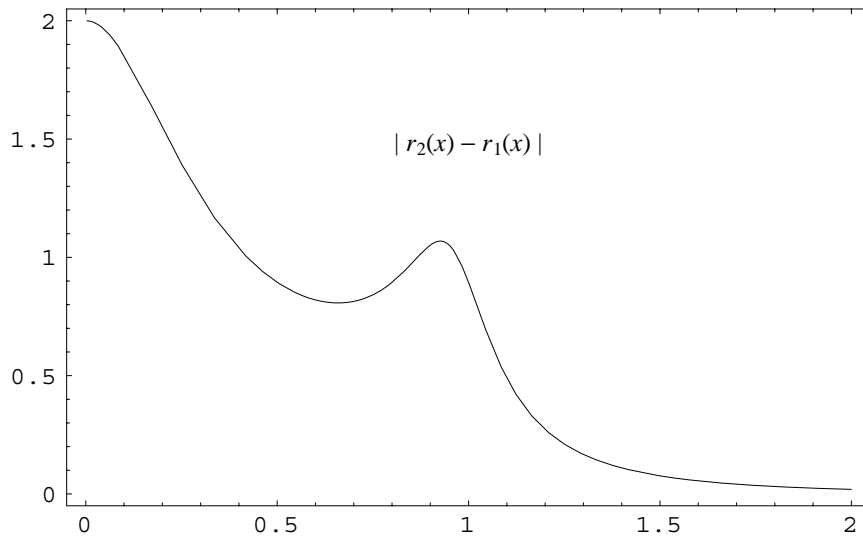


FIG. 7. $|r_1(x) - r_2(x)|$ for Example 16. Since $C = 2 \gg 0$, $|r_1(x) - r_2(x)|$ is large throughout $[0, 1]$, so for small ω , the low order Josephson junction eigenvalues $r_2(j\omega)$ are far from the corresponding forced pendulum eigenvalues $r_1(j\omega)$.

$[0.75, 0.8]$, while $I(\omega)$ is in $[0.54, 0.58]$.

The dissimilarity is not surprising since, for *all* small ω , the low order eigenvalues $r_2(j\omega)$ are far from $r_1(j\omega)$ for $j = 1, 2, \dots$ up to, say, $j \leq 1/\omega$ (Figure 7). This situation should be contrasted with Example 15, in which the Josephson junction and pendulum eigenvalues are all close *except* near the frequencies $\omega = 1/2k$, where *one* (the $2k$ th) pair of the Josephson and pendulum eigenvalues differ significantly.

Figure 9 shows a close-up view of the $I(\omega)$ graph for $0.95 < \omega < 1.4$, which includes the first place where $I(\omega)$ is decreasing. At $I = 1.37$, there are three SWFSs with frequencies $\omega = 0.978\dots, 1.09\dots, 1.22\dots$, and the periodic pendulum solution has frequency $1.3245\dots$. Table 3 lists the Fourier coefficients for these waveforms through $M = 8$, and the waveforms are displayed in Figure 10.

The effect of truncating the Fourier series when computing $I(\omega)$ is shown in Figure 11 in which $I(\omega)$, for $0.15 < \omega < 0.4$, has been computed using $M = 5$, $M = 6$, and $M = 7$. At the resolution of the graph, the curves begin to separate at about $\omega = 0.27$, and continue separating as ω decreases. The hump around $\omega = 0.16$ is absent in the computation with $M = 5$; this suggests that the nonmonotonicity at that hump is related to the sixth eigenvalue $\lambda_6(\omega)$, which, of course, is not present when $M = 5$.

The last graph (Figure 12) shows $I(\omega)$, computed with $M = 12$, on the interval $[0.10, 0.14]$. The damped oscillatory behavior of $I(\omega)$ continues down to $\omega = 0.10$; in particular, with $I = 0.55$, there are fourteen SWFSs, with distinct frequencies $\omega > 0.10$, to the Josephson junction system of Example 16, and most likely, many more with $\omega < 0.1$. However the numerical method alone is insufficient to ascertain the exact nature of $I(\omega)$ as $\omega \rightarrow 0$, since the number M of Fourier terms must be increased without a bound as ω approaches 0.

The computations and graphs presented above were produced by *Mathematica*

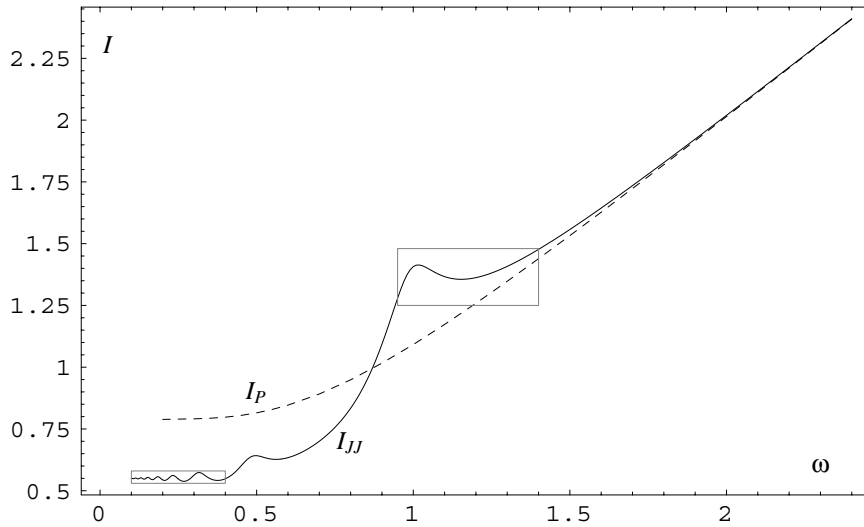


FIG. 8. $I(\omega)$, for $0.1 < \omega < 2.4$, for the Josephson junction system of Example 16: $\beta = 2$; $L = 1$, $R = 0.0001$, $C = 2$; $N = 1$; and $I_P(\omega)$ for $\beta = 2$. The enclosed regions are blown up in Figures 9 and 12. In contrast to Example 15, the I_{JJ} and I_P curves show almost no relationship to each other once they separate. The number M of Fourier terms increases from 4 to 12 as ω decreases from 2.4 to 0.1; $\Delta\omega$ varies between 0.05 and 0.001.

TABLE 3

Frequencies and Fourier coefficients for the three SWFSs of the Josephson junction system at $I = 1.37$ with parameters in Example 2 ($\beta = 2$; $L = 1$, $R = 0.0001$, $C = 2$; $N = 1$) and (fourth column) for the periodic forced pendulum solution at $\beta = 2$, $I = 1.37$.

ω	0.978288	1.09252	1.2344	1.32453
a_1	0.859392	0.587644	0.300832	0.0915033
b_1	-0.219456	0.396063	0.383768	0.244867
a_2	0.0498767	0.0352847	0.0163448	0.00468193
b_2	-0.0294711	0.0117363	0.0131341	0.00772108
a_3	-0.00258919	0.00325108	0.00142819	0.000284968
b_3	-0.00518855	-0.00139313	0.000300498	0.000286578
a_4	-0.000656393	0.000168706	0.000109986	0.0000174293
b_4	0.0000614755	-0.000326329	-0.0000289178	0.0000104365
a_5	-0.0000228109	-8.08971×10^{-6}	7.12982×10^{-6}	41.04476×10^{-6}
b_5	0.0000826832	-0.0000402704	-6.21608×10^{-6}	3.08624×10^{-7}
a_6	9.57267×10^{-6}	-3.65614×10^{-6}	3.15186×10^{-7}	6.0832×10^{-8}
b_6	6.65681×10^{-6}	-3.08486×10^{-6}	-7.55867×10^{-7}	2.03591×10^{-9}
a_7	1.3281×10^{-6}	-5.72052×10^{-7}	-4.604256×10^{-9}	3.4133×10^{-9}
b_7	-9.17643×10^{-7}	-1.72142×10^{-8}	-7.27361×10^{-8}	-7.66973×10^{-10}
a_8	-5.56046×10^{-8}	-5.60165×10^{-8}	-3.29468×10^{-9}	1.82466×10^{-10}
b_8	-2.22023×10^{-7}	4.1689×10^{-8}	-5.73832×10^{-9}	-9.40311×10^{-11}

3.0 running on a desktop PowerMac. A *Mathematica* notebook containing functions which implement the numerical methods of this section may be obtained from the authors, as well as notebooks with the particular computations in the two examples.

5. Conclusion. We have presented a new proof of existence of SWFSs for series arrays for Josephson junctions and employed the methods of this proof to establish the uniqueness of these waveforms when either the bias current I or number of junctions

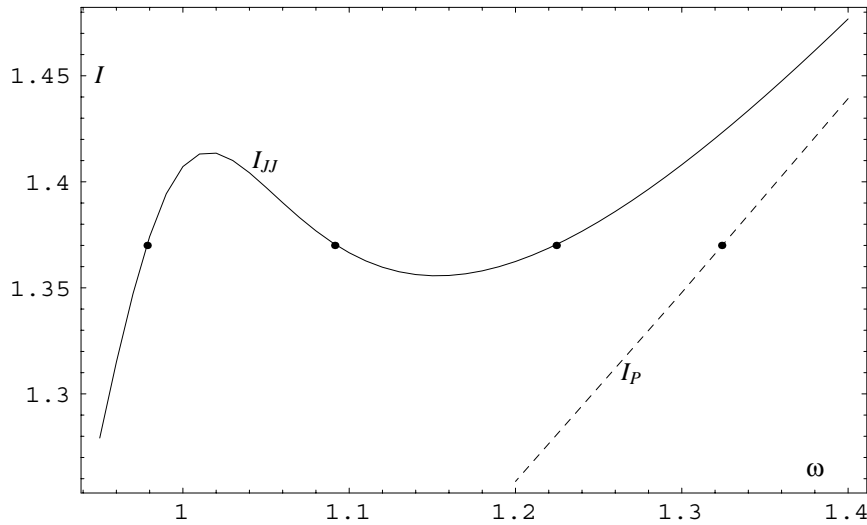


FIG. 9. Close-up on Figure 8, showing I_{JJ} and I_P for $0.95 < \omega < 1.4$. The dots are at $I = 1.37$, at which the Josephson junction system of Example 16 admits three SWFSs with frequencies 0.97829, 1.0925, and 1.2234. The periodic pendulum solution with $\beta = 2$, $I = 1.37$ has frequency $\omega = 1.32453$.

N is sufficiently large. For N large, the equations that determine the SWFS, when formulated as a fixed point equation on a Hilbert space, converge in a way that we made precise to the analogous but simpler fixed point equation for periodic solutions to the forced nonlinear pendulum. This equation is known to have a unique periodic solution (for $I > 1$), but in fact we established this as a by-product of our methods.

We then outlined a strategy for finding parameter lists for which the Josephson junction system (1) has multiple SWFSs and described how to find these numerically. Our method is essentially to use Newton's method to find the Fourier coefficients of the wave forms. We gave examples of Josephson junction systems which possess many distinct SWFSs. Admittedly, our numerical work is not a proof that SWFSs exist, but we consider our numerical evidence extremely compelling.

We close with some open questions and suggestions for future research. In our numerical work we graph I as a (single-valued) function of ω , but in fact we do not know whether there are parameter values for which I is multivalued. In other words, we do not know whether the equation $f = \mathcal{L}_\omega \mathcal{S}(f)$, which gives SWFSs to (1) for *unspecified* I , has a unique solution for any given $\omega > 0$. This assertion is true for the pendulum problem; see [LHM] for the proof. Equivalently, we do not know whether (1) (with unspecified I) can ever admit two distinct SWFSs with the *same* frequency.

We are also intrigued by the behavior of $I(\omega)$ as $\omega \rightarrow 0$. For the pendulum problem, $I(\omega)$ is always monotonic, and so there is a limiting value $I_0 = \lim_{\omega \rightarrow 0} I(\omega)$ below which no periodic running solutions exist. Furthermore, the bifurcation at I_0 can be described fairly easily (see [LHM]). In our case, it seems that the graph of $I(\omega)$ has infinitely many ripples as $\omega \rightarrow 0$, which suggests that the bifurcation at the limiting value I_0 (if it exists) may be extremely complicated. For the special cases $L = R = 0$ or $L = C^{-1} = 0$ and in-phase SWFSs, this analysis has been completely carried out in [AGK], where it is shown that the bifurcation behavior is reasonably

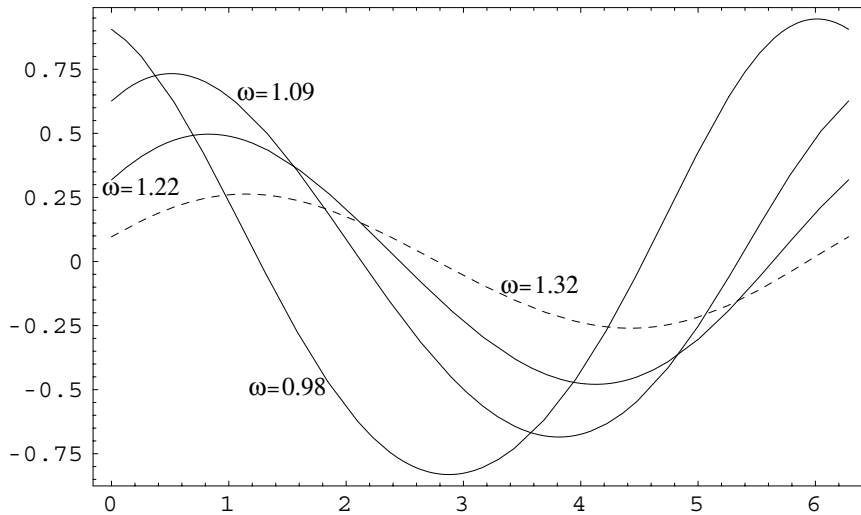


FIG. 10. Waveforms $f(t)$, on $[0, 2\pi]$, for the three SWFs to the Josephson junction system with parameters $\beta = 2$; $L = 1$, $R = 0.0001$, $C = 2$; $I = 1.37$; $N = 1$ (the solid curves). The dashed curve is the waveform for the periodic solution of the forced pendulum equation with $\beta = 2$, $I = 1.37$.

tame. But as we saw in our numerical work, nonmonotonicity is essentially an LC phenomenon, so the behavior of the bifurcation when both L and C are positive may be much different.

Many researchers have considered Josephson junction arrays with more complicated topologies than series arrays, which are essentially coupled “all-to-all.” Some of the most interesting recent work in Josephson junctions concerns junctions coupled in chains, ladders, rings, or double rings; see [VBD], [WVS], [DTO], [DWO], and [BTO]. We suspect that our methods will apply to these networks, so that existence or uniqueness results for various parameter ranges can be established.

Also of interest to us is the question of the dynamic stability of SWFs to Josephson junction arrays. SWFs may be stable, unstable, or neutrally stable in terms of the dynamics of the Josephson junction system. Aronson, Golubitsky, and Krupa established this for in-phase solutions in [AGK], and Nichols, Wiesenfeld [NW] and Watanabe, Swift [WSw] gave examples of unstable SWFs with all junctions distinct in phase (the case considered in this paper). The case when $\beta = 0$ has been thoroughly analyzed; in this case, SWFs are neutrally stable in all but 4 directions (see [TS], [TMS], [WSt], and [SM]).

Our examples of multiple SWFs give another demonstration that unstable SWFs exist, since these multiple SWFs are born in a tangent bifurcation, and so at least one must be unstable. This raises an intriguing question, asked by Steve Strogatz: When multiple SWFs exist, are *any* of the SWFs stable? (He thinks not.) In the general case when $\beta > 0$ the stability problem is open. We think there might be some hope of understanding stability in the general case as $N \rightarrow \infty$, since now we at least know that the SWF is unique for N large. We hope to work on this in the future.

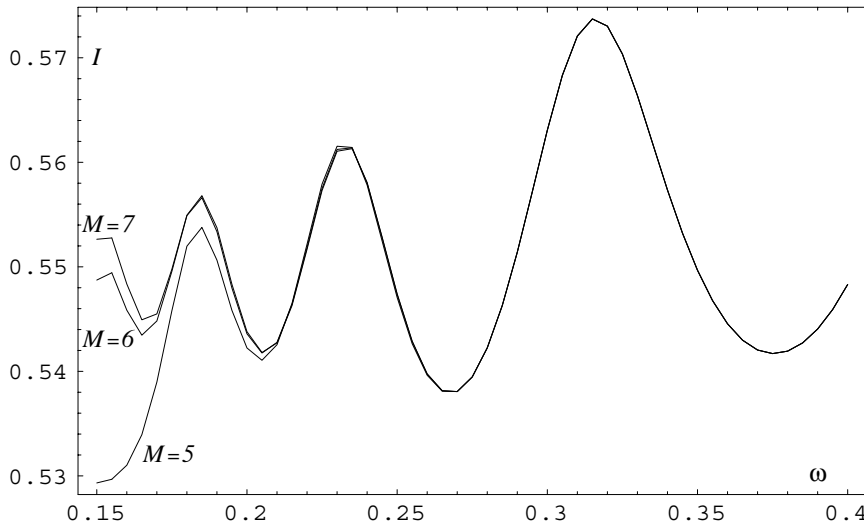


FIG. 11. The effect of truncation on the computation of $I(\omega)$ for the parameters of Example 16. The three curves were computed using $M = 5, 6, 7$ over $0.15 < \omega < 0.4$ with $\Delta\omega = 0.05$. They are indistinguishable for $\omega > 0.27$, but completely different by $\omega = 0.15$. The hump which peaks around 0.16 is missing when $M = 5$, suggesting that it is related to the sixth eigenvalue $\lambda_6(\omega) = r_2(6\omega)$, which, for ω near 0.16, behaves like $r_2(x)$ near $x = x_1 = 1$.

Appendix.

LEMMA 17. Let $F_n, F : U \rightarrow K \subset U$ be continuously differentiable maps where K is compact and U is an open subset U of a Banach space X . Assume $F_n \rightarrow F$ and $DF_n \rightarrow DF$ uniformly on U . Suppose that F has a unique fixed point which is nondegenerate. Then F_n has a unique fixed point for all sufficiently large n .

Proof. Let $x_0 \in K$ be the unique fixed point of F and let $A = DF(x_0)$. Then $(I - A)^{-1}$ exists and is bounded, so we can form the functions

$$G_n(x) = x - (I - A)^{-1}(x - F_n(x)),$$

$$G(x) = x - (I - A)^{-1}(x - F(x)).$$

Observe that $G_n \rightarrow G$ and $DG_n \rightarrow DG$ uniformly on U . We also see that G_n and F_n have exactly the same fixed points, and that G has the unique fixed point x_0 . In addition, $DG(x_0) = 0$. We can find some $r > 0$ such that $\|DG(x)\| \leq 1/3$ for all $x \in \overline{B}_r(x_0) \subset U$, where $\overline{B}_r(x_0)$ is the closed ball of radius r centered at x_0 . Then we can find some N such that $n \geq N$ implies $\|DG_n(x)\| \leq 1/2$ for all $x \in \overline{B}_r(x_0)$. We can also assume that $\|G_n(x) - G(x)\| \leq r/2$ for $n \geq N$ and $x \in \overline{B}_r(x_0)$, since $G_n \rightarrow G$ uniformly on U . This gives

$$\begin{aligned} \|G_n(x) - x_0\| &\leq \|G_n(x) - G(x)\| + \|G(x) - G(x_0)\| \\ &\leq \frac{r}{2} + \frac{1}{2}\|x - x_0\| \\ &\leq r \end{aligned}$$

for any $x \in \overline{B}_r(x_0)$ and $n \geq N$ (here we used $G(x_0) = x_0$ and the usual derivative estimate for $\|G(x) - G(x_0)\|$). This proves that G_n maps $\overline{B}_r(x_0)$ to itself for $n \geq N$.

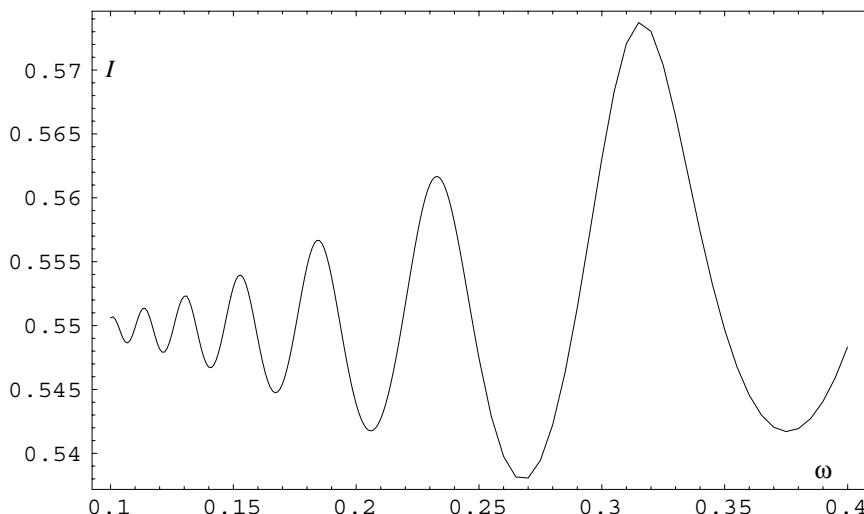


FIG. 12. Close-up of Figure 8, showing $I(\omega)$ for Example ?? on $[0.1, 0.4]$, computed with $M = 8$, $\Delta\omega = 0.05$ (for $\omega > 0.25$) and $M = 12$, $\Delta\omega = 0.001$ (for $\omega < 0.25$). There are 14 frequencies for which $I(\omega) = 0.55$.

Since $\|DG_n(x)\| \leq 1/2$ for $x \in \overline{B}_r(x_0)$ and $n \geq N$, we see that G_n is a contraction map on $\overline{B}_r(x_0)$, and so G_n , and hence F_n , must have a unique fixed point in $\overline{B}_r(x_0)$, for $n \geq N$.

Now we show that any fixed point of F_n must lie in $B_r(x_0)$ if n is sufficiently large. Any fixed points must lie in K . The function $x \mapsto \|F(x) - x\|$ is continuous on the compact set $K - B_r(x_0)$ and is never 0. Hence we can find an $m > 0$ such that $\|F(x) - x\| \geq m$ for all $x \in K - B_r(x_0)$. So for n sufficiently large we have $\|F_n(x) - x\| \geq m/2$ for all $x \in K - B_r(x_0)$. Therefore any fixed point of F_n must lie in $B_r(x_0)$. Hence we see that F_n has a unique fixed point in U for n sufficiently large. \square

LEMMA 18. Let $F : U \times (a, b) \rightarrow K \subset U$ be a continuously differentiable map where K is compact and U is an open subset U of a Banach space X . For any $c \in (a, b)$, define $F_c : U \rightarrow K$ by the rule $F_c(x) = F(x, c)$. Suppose all fixed points of F_c are nondegenerate for all $c \in (a, b)$. Then the number of fixed points of F_c is finite and constant as a function of c .

Proof. All fixed points of F_c lie in K , so suppose $x_0 \in K$ is a fixed point of F_{c_0} , for some $c_0 \in (a, b)$. Imitating the proof of Lemma 17, we let $A = DF_{c_0}(x_0)$ and form the function

$$G_c(x) = x - (I - A)^{-1}(x - F_c(x))$$

for $x \in U$ and $c \in (a, b)$. Then F_c and G_c have the same fixed points and $DG_{c_0}(x_0) = 0$. Since F is continuously differentiable, G_c is continuously differentiable in x and c so there exist $r, \delta > 0$ such that

$$\|DG_c(x)\| \leq \frac{1}{2} \quad \text{and} \quad \|\dot{G}_c(x) - \dot{G}_{c_0}(x_0)\| \leq 1$$

if $\|x - x_0\| \leq r$ and $|c - c_0| \leq \delta$, where dot denotes differentiation with respect to c . Consequently

$$\|\dot{G}_c(x)\| \leq \|\dot{G}_{c_0}(x_0)\| + 1$$

if $\|x - x_0\| \leq r$ and $|c - c_0| \leq \delta$. Therefore we can find a constant $M > 0$ such that if $\|x - x_0\| \leq r$ and $|c - c_0| \leq \delta$, then $\|\dot{G}_c(x)\| \leq M$. For such x, c we have

$$\|G_c(x) - G_{c_0}(x_0)\| \leq \|G_c(x) - G_{c_0}(x)\| + \|G_{c_0}(x) - G_{c_0}(x_0)\|.$$

Now $G_{c_0}(x_0) = x_0$, and the standard derivative estimates (in c and x , respectively) give

$$\begin{aligned} \|G_c(x) - x_0\| &\leq M|c - c_0| + \frac{1}{2}\|x - x_0\| \\ &\leq M\delta + \frac{1}{2}r \end{aligned}$$

if $\|x - x_0\| \leq r$ and $|c - c_0| \leq \delta$. By shrinking δ if necessary, we can assume that $M\delta \leq r/2$, so we conclude that $\|G_c(x) - x_0\| \leq r$ provided that $\|x - x_0\| \leq r$ and $|c - c_0| \leq \delta$. As before, this shows that G_c maps the closed ball $\overline{B}_r(x_0)$ to itself if $|c - c_0| \leq \delta$ and is a contraction map since $\|DG_c(x)\| \leq 1/2$ for $x \in \overline{B}_r(x_0)$. Hence G_c , and therefore F_c , has a unique fixed point in $\overline{B}_r(x_0)$ if $|c - c_0| \leq \delta$. In particular all fixed points of F_c are isolated, and so for any given c , F_c can have at most finitely many fixed points because all fixed points lie in the compact set K .

Now fix $c_0 \in (a, b)$, and suppose F_c has fixed points x_1, x_2, \dots, x_k . We can find $r, \delta > 0$ as above, so that F_c has a unique fixed point in $\overline{B}_r(x_i)$, $i = 1, 2, \dots, k$ if $|c - c_0| \leq \delta$. We must show that F_c has no other fixed points if c is sufficiently close to c_0 . Then for such c , F_c has exactly k fixed points, so the number of fixed points is locally constant, and hence constant, on the interval (a, b) .

The function $x \mapsto \|F_{c_0}(x) - x\|$ is nonzero on the compact set

$$K' = K - (B_r(x_1) \cup \dots \cup B_r(x_k)),$$

so there is some $m > 0$ such that $x \in K' \Rightarrow \|F_{c_0}(x) - x\| \geq m$. Since K' is compact and F_c is continuous in x and c , we have $\|F_c(x) - x\| \geq m/2$ for all $x \in K'$ provided that $|c - c_0|$ is sufficiently small. In particular, if F_{c_0} has no fixed points, then $K' = K$ and F_c has no fixed points if $|c - c_0|$ is sufficiently small. Therefore the number of fixed points is locally constant as a function of c , and we're done. \square

Acknowledgments. We wish to acknowledge a great debt to the work of Aronson and Huang. Their seminal paper influenced us to think about these questions, and our approach is in many ways inspired by their work. We also thank Steve Strogatz, who read a preliminary version of this work and made many useful suggestions, and the referees for their helpful comments.

REFERENCES

- [AGK] D. G. ARONSON, M. GOLUBITSKY, AND M. KRUPA, *Coupled arrays of Josephson junctions and bifurcation of maps with S_N symmetry*, *Nonlinearity*, 4 (1991), pp. 861–902.
- [AGM] D. G. ARONSON, M. GOLUBITSKY, AND J. MALLETT-PARET, *Ponies on a merry-go-round in large arrays of Josephson junctions*, *Nonlinearity*, 4 (1991), pp. 903–910.
- [AH1] D. G. ARONSON AND Y. S. HUANG, *Limits and uniqueness of discrete rotating waves in large arrays of Josephson junctions*, *Nonlinearity*, 7 (1994), pp. 777–804.

- [AH2] D. G. ARONSON AND Y. S. HUANG, *Single wave-form solutions for linear arrays of Josephson junctions*, Phys. D, 101 (1997), pp. 157–177.
- [BTO] M. BARAHONA, E. TRÍAS, T. P. ORLANDO, A. E. DUWEL, H. S. J. VAN DER ZANT, S. WATANABE, AND S. H. STROGATZ, *Resonances of dynamical checkerboard states in Josephson arrays with self-inductance*, Phys. Rev. B, 55 (1997), pp. 989–992.
- [DTO] A. E. DUWEL, E. TRÍAS, T. P. ORLANDO, H. S. J. VAN DER ZANT, S. WATANABE, AND S. H. STROGATZ, *Resonance splitting in discrete planar arrays of Josephson junctions*, J. Appl. Phys., 79 (1996), pp. 7864–7870.
- [DWO] A. E. DUWEL, S. WATANABE, E. TRÍAS, T. P. ORLANDO, H. S. J. VAN DER ZANT, AND STEVEN H. STROGATZ, *Discreteness-induced resonances and AC voltage amplitudes in long one-dimensional Josephson junction arrays*, J. Appl. Phys., 82 (1997), pp. 4661–4668.
- [HA] Y. S. HUANG AND D. G. ARONSON, *Discrete rotating wave solutions for system of globally coupled Josephson junctions*, Internat. J. Bifur. Chaos, 6 (1996), pp. 1789–1797.
- [LHM] M. LEVI, F. C. HOPPENSTEADT, AND W. L. MIRANKER, *Dynamics of the Josephson junction*, Quart. Appl. Math., 36 (1978), pp. 167–198.
- [L] K. K. LIKHAREV, *Dynamics of Josephson Junctions and Circuits*, Gordon and Breach, New York, 1986.
- [M] R. E. MIROLLO, *Splay-phase orbits for equivariant flows on tori*, SIAM J. Math. Anal., 25 (1994), pp. 1176–1180.
- [NW] S. NICHOLS AND K. WIESENFELD, *Ubiquitous neutral stability of splay-phase states*, Phys. Rev. A, 45 (1992), pp. 8430–8435.
- [OD] T. P. ORLANDO AND K. A. DELIN, *Foundations of Applied Superconductivity*, Addison-Wesley, Reading, MA, 1991.
- [Ru] W. RUDIN, *Functional Analysis*, 2nd ed., McGraw-Hill, New York, 1991.
- [S] S. H. STROGATZ, *Nonlinear Dynamics and Chaos*, Addison-Wesley, Reading, MA, 1994.
- [SM] S. H. STROGATZ AND R. E. MIROLLO, *Splay states in globally coupled Josephson arrays: Analytical prediction of Floquet multipliers*, Phys. Rev. E, 47 (1993), pp. 220–227.
- [TS] K. Y. TSANG AND I. B. SCHWARZ, *Interhyperhedral diffusion in Josephson junction arrays*, Phys. Rev. Lett., 68 (1992), pp. 2265–2268.
- [TMS] K. Y. TSANG, R. E. MIROLLO, S. H. STROGATZ, AND K. WIESENFELD, *Dynamics of a globally coupled oscillator array*, Phys. D, 48 (1991), pp. 102–112.
- [VBD] H. S. J. VAN DER ZANT, M. BARAHONA, A. E. DUWEL, E. TRÍAS, T. P. ORLANDO, S. WATANABE, AND S. H. STROGATZ, *Dynamics of one dimensional Josephson junction arrays*, Phys. D, 1994 (1998), pp. 1–8.
- [VT] T. VAN DUZER AND C. W. TURNER, *Principles of Superconducting Devices and Circuits*, Elsevier, New York, 1981.
- [WSt] S. WATANABE AND S. H. STROGATZ, *Constants of motion for superconducting Josephson arrays*, Phys. D, 74 (1994), pp. 197–253.
- [WSw] S. WATANABE AND J. W. SWIFT, *Stability of periodic solutions in series arrays of Josephson junctions with internal capacitance*, J. Nonlinear Sci., 7 (1997), pp. 503–536.
- [WVS] S. WATANABE, H. S. J. VAN DER ZANT, S. H. STROGATZ, AND T. P. ORLANDO, *Dynamics of circular arrays of Josephson junctions and the discrete Sine-Gordon equation*, Phys. D, 97 (1996), pp. 429–470.